creative commons
COMMONS DEED

저작자표시-비영리-변경금지 2.0 대한민국

이용자는 아래의 조건을 따르는 경우에 한하여 자유롭게

- 이 저작물을 복제, 배포, 전송, 전시, 공연 및 방송할 수 있습니다.

다음과 같은 조건을 따라야 합니다:

저작자표시. 귀하는 원저작자를 표시하여야 합니다.

비영리. 귀하는 이 저작물을 영리 목적으로 이용할 수 없습니다.

변경금지. 귀하는 이 저작물을 개작, 변형 또는 가공할 수 없습니다.

- 귀하는, 이 저작물의 재이용이나 배포의 경우, 이 저작물에 적용된 이용허락조건을 명확하게 나타내어야 합니다.
- 저작권자로부터 별도의 허가를 받으면 이러한 조건들은 적용되지 않습니다.

저작권법에 따른 이용자의 권리는 위의 내용에 의하여 영향을 받지 않습니다.

이것은 이용허락규약(Legal Code)을 이해하기 쉽게 요약한 것입니다.

Disclaimer

dCollection

의학박사 학위논문

Noradrenergic Regulation of Neuroglia Interaction is Essential for Proper Cerebellar Output and Cerebellum-Dependent Motor Coordination

소뇌 출력과 운동협응에 있어서 노르아드레날린에 의한 신경-아교세포 상호작용조절의 중요성에 대한 연구

2015 년 2 월

서울대학교 대학원

의과학과 신경생리학전공

노 승 언

A thesis of the Degree of Doctor of Philosophy

소뇌 출력과 운동협응에 있어서 노르아드레날린에 의한 신경-아교세포 상호작용조절의 중요성에 대한 연구

Noradrenergic Regulation of Neuroglia Interaction is Essential for Proper Cerebellar Output and Cerebellum-Dependent Motor Coordination

February 2015

The Department of Biomedical Sciences

Seoul National University

College of Medicine

Seung-Eon Roh

ABSTRACT (IN ENGLISH)

BACKGROUND: Locus coeruleus (LC)-norepinephrine (NE) system exerts prominent effects on neurons and astrocytes in many brain regions, including the cerebellum, thereby contributing to arousal. However, the possible NE-driven interaction between neurons and glia in the cerebellum and its physiological role during arousal remains to be understood.

MATERIALS AND METHODS: To visualize the Ca^{2+} activity of Purkinje cell (PC), molecular layer interneuron (MLI) and Bergmann glia (BG) in intact cerebellar cortex lobule V/VI, two-photon calcium imaging using a calcium dye OGB-1 and genetically encoded calcium indicator GCaMP6f (viral expression) was performed in anesthetized and awake head-fixed mice. Noxious electrical stimuli was delivered to anesthetized mice and startle stimuli to resting awake mice during two-photon imaging to induce arousal-like state and arousal behavior, respectively.

RESULTS: 1) Noxious electrical stimulation in anesthetized mice or startle stimulation in awake mice results in NE release and subsequent BG Ca^{2+} response in the cerebellum. 2) The BG Ca^{2+} response coincides with phasic suppression of PC dendritic calcium spike activity during electrical stimulation in anesthetized mice and during arousal behavior in awake mice. 3) Cerebellum specific blockades of both alpha1-adrenergic receptor (AR) and glial GABA channel, Best1, result in abnormally elevated network synchrony and increased Ca^{2+} transients in PC dendrites during resting and arousal state: aberrantly increased PC output. 4) alpha1-AR and Best1 blockade induce locomotion disability and dystonic behavior which was coincided with PC burst activity.

CONCLUSION: Taken together, it is suggested that NE-driven inhibitory gliotransmission mediates suppression of PC dendritic Ca^{2+} activity and it supports proper PC output and cerebellum-dependent motor coordination, otherwise inducing dystonic behavior.

Keywords: Cerebellum, Norepinephrine, Locus Coeruleus, Calcium, Bergmann Glia, Purkinje Cell, Neuroglia interaction, Motor coordination, Dystonia

Student number: 2010-30609

CONTENTS

LIST OF TABLES AND FIGURES

LIST OF ABBREVIATIONS

AR: Adreno-receptor or adrenergic receptor

BG: Bergmann glia

BGCR: BG Ca^{2+} response

ES: Electrical stimulation

GECI: Genetically encoded calcium indicator

HL: Hind limb

HPES: Hind-paw ES

LC: Locus coeruleus

ML: Molecular layer

MLI: Molecular layer interneuron

NE: Norepinephrine

OGB-1/AM: Oregon green BAPTA-1 aceto-methyl

PC: Purkinje cell

PCL: Purkinje cell layer

PO day: Post-operation day

ROI: Region of interest

SR101: Sulfo-rhodamine101

TG: Transgenic

INTRODUCTION

Traditionally, cerebellum is involved in sensory integration and motor coordination (Fine et al., 2002), non-motor functions more recently being described (Strick et al., 2009). There are two major inputs, climbing fiber from inferior olive and parallel fiber from granule cells, which stimulate Purkinje cell (PC), the sole output of the cerebellum (Ramnani, 2006). Another relatively less known afferent, the noradrenergic afferent projects from locus coeruleus (LC) and releases norepinephrine (NE) throughout all layers of cerebellum (Bloom et al., 1971; Kimoto et al., 1978), in which they use volume transmission in non-synaptic junctions to activate adrenergic receptors (AR) (Abbott and Sotelo, 2000). Though the role of LC has been established as pain modulation (Pertovaara, 2006), circadian regulation (Gonzalez and Aston-Jones, 2006), and maintenance of behavioral states of high arousal (Aston-Jones and Cohen, 2005), the regulatory mechanism of NE on cerebellar circuit and its physiological role in LC-related motor response remains to be investigated.

LC-NE system is known to facilitate both excitatory and inhibitory tones of evoked responses in target areas (Waterhouse et al., 1980; Waterhouse and Woodward, 1980) and this is also true for cerebellum as revealed by electrophysiological studies *in vitro* and *in vivo*. Importantly, direct electrical stimulation of LC results in NE release in cerebellum (Bickford-Wimer et al., 1991). One of the prominent features of NE effect on cerebellar circuit is the facilitation of GABA transmission and subsequent suppression of PC activity

(Parfitt et al., 1988). As for the receptor subtypes involved, α- and β-AR agonists suppress PC firing rate and corresponding antagonists block the NE-mediated suppression (Parfitt et al., 1988). Mechanistically, it was dependent on post-synaptic events (Cheun and Yeh, 1992; Moises et al., 1979; Waterhouse et al., 1984) and pre-synaptic processes mediated by β-AR-mediated augmentation of GABAergic transmission at PC-interneuron synapses (Saitow et al., 2000) or by α2-AR-mediated decrease in release probability in PC-climbing fiber (CF) synapses (Carey and Regehr, 2009). As such, the effect of NE on cerebellar circuitry looks considerable. Notably, a relatively unknown down-stream effector of NE effect is the α1-AR which mediates an increase of spontaneous synaptic inhibition of PC (Herold et al., 2005; Hirono and Obata, 2006). α1-AR expression and following Ca^{2+} response is exclusively reported in Bergmann glia (BG), a type of glial cell located in PC and molecular layer (Kirischuk et al., 1996; Kulik et al., 1999). Recently, the BG Ca^{2+} response sensitive to α1-AR antagonist was observed in behaving mice and was suggested to mediate astroglial responsiveness to local circuit activity during behaviorally triggered arousal responses (Paukert et al., 2014).

It has been established that in many brain areas glial cells participate in modulation of morphology and function of neurons, glia calcium elevation being an important feature (Kang et al., 1998; Lalo et al., 2014; Newman and Zahs, 1998; Poskanzer and Yuste, 2011; Torres et al., 2012). In cerebellum, accumulative evidence indicate the capability of BG to regulate the PC activity by glutamatergic signaling (Brockhaus and Deitmer, 2002) and glial Ca^{2+}-dependent extracellular K^+ uptake (Wang et al., 2012). Outstandingly, BG

optogenetic stimulation drives PC activity and promptly perturbs cerebellar motor behavior (Sasaki et al., 2012). As such, BG receives remarkable attention in regulating neuronal function and related behavior.

Here, I provide a series of evidence that NE participates in BG-PC interaction in which PC dendritic Ca^{2+} activity is suppressed by inhibitory gliotransmission in order to generate proper output for motor coordination. Using two-photon calcium imaging technique utilizing the chemical Ca^{2+} dye OGB-1/AM and recently developed genetically encoded calcium indicator (GECI) GCaMP6f, the activity of various cell types, BG, MLI and PC, were visualized. The α1-AR-dependent BG Ca^{2+} response was coincided with PC dendritic Ca^{2+} activity suppression by peripheral noxious electrical stimulation and arousal stimuli in anesthetized mice and awake behaving mice, respectively. The pharmacological blockades of α1-AR resulted in abnormally enhanced synchronous activity of PC activity, which was reproduced by glial GABA channel Best1 inhibition. Hence, I suggest that NE-driven inhibitory gliotransmission plays critical role in supporting proper cerebellar output for motor coordination.

MATERIALS AND METHODS

Animals and craniotomy surgery

The experimental processes were approved by the Seoul National University Institutional Animal Care and Use Committee and performed in accordance with the guidelines of the National Institutes of Health. 7-10 week old C57BL/6J mice were anesthetized by inhalation of isoflurane (3% for induction and 1-1.5% during experiment) in pure O_2 or intraperitoneal injection of Zoletil/Rompun mixture (30mg/10mg/kg). A small craniotomy was made over the lobule IV/V cerebellar vermis according to the previous descriptions with some modifications (Carrillo et al., 2013; Kim and Nabekura, 2011; Ozden et al., 2012). In short, after placing the anesthetized mouse on stereotaxic frame (Narishige, Tokyo, Japan), skin was incised and bone was removed by dental drill and No.5 surgical knife. In order to minimize the edema and related inflammation, dexamethasone (0.2mg/kg) and meloxicam (20mg/kg) were administered by subcutaneous injection. After calcium dye or virus injection, 1.2 × 2.2 or 1.3 × 2.3 mm size glass coverslip (Matsunami, Japan) was tightly placed on the cerebellar cortex and fixed by applying cyanoacrylate glue (Vetbond, 3M). A metal ring for head fixation was attached by dental cement, Superbond (Sun Medical, Japan). For OGB-1/AM acute imaging, low melting typeIII agarose (Sigma) was between cover glass and cortex to reduce pulsation and breathing induced motion artifacts. For drug application, glass coverslip was placed on the cortex and partially sealed using cyanoacrylate glue. For cre-

dependent Purkinje cell specific expression of GCaMP6f, pcp2-cre transgenic mouse was used (Jackson Lab, US).

Chemical calcium indicator

For acute calcium imaging of PC and/or BG, we used Oregon Green BAPTA1-AM (Invitrogen, CA) (Kitamura and Hausser, 2011) together with sulfo-rhodamine 101 (SR-101, Sigma) which specifically stains Bergmann Glia (Hoogland et al., 2011; Nimmerjahn et al., 2009). 5 μl of fluronic F-127 (Invitrogen, CA) in 20% DMSO was added to a single vial of 10 μg OGB-1/AM. After vortexing, 51.25 μl of ACSF (135mM NaCl, 2.7mM KCl, 1mM $MgCl_2$, 1.8mM $CaCl_2$, 5mM HEPES, pH 7.4) and 6.25 μl SR101 (1mM) was were added, sonicated and filtered with 0.22 μm disposable pore filter (Toyo Roshi Kaisha, Japan). During acute OGB-1 imaging, urethane (1.2g/kg) supplemented with atropine (0.02mg/kg) was generally used. The freshly prepared dye mixture was pressure injected with picopump (WPI, FL) with 10-20 psi into the exposed cerebellar cortex using beveled glass micropipette (5 MΩ). After 30-40 min for diffusion and staining of the dye, imaging of PC and/or BG was performed by two-photon microscopy.

Simultaneous neurogila calcium measurement by GCaMP6f chronic window imaging

For cre-dependent specific expression of GCaMP6f in PC, we pressure injected 1/5 diluted solution of AAV1.CAG.Flex.GCaMP6f.WPRE.SV40 (UPenn Vector Core, PA) in pcp2-cre TG mouse. AAV1.CAG.GCaMP6f.WPRE.SV40

was used in wild-type mouse for expression in PC, BG, and MLI. Consistent with a previous report (Najafi et al., 2014), the baseline expression of GCaMP6f was almost exclusively present in PC and rare in BG and MLI of which spontaneous calcium activity was not seen during anesthesia. However, during awake imaging, calcium excitation of MLI and BG was observed, consequently enabling imaging calcium transients of PC, MLI and BG at the same time.

Two-photon microscopy and image acquisition

Confocal microscopy was performed with laser scanning multiphoton microscope (Zeiss LSM 7 MP, Carl Zeiss, Jena, Germany). Excitation was carried out by a mode-locked titanium:sapphire laser system (Chameleon, Coherent, Santa Clara, CA, USA) operating the wavelength at 850 nm for OGB-1 and 900nm for GCaMP6f imaging. For SR101 signal detection, two-channel (GFP and RFP) imaging was performed. Generally, objective W Plan-Apochromat 20×, 1.0 numerical aperture (Carl Zeiss) was used. Images were acquired using ZEN software (Zeiss Efficient Navigation, Carl Zeiss) and processed using MATLAB (MathWorks). For every run of imaging, a high-resolution reference image was acquired (512 × 512, 8 sec per a frame) in PC layer (120 – 150 μm from dura) and molecular layer (around 100 - 50 μm from dura). For PC or PC-BG simultaneous calcium recording, 512 × 128 or 256 × 64 resolution time-lapse imaging was performed at a speed of 200 or 125 ms per a frame resulting in 5 or 8 Hz of sampling rate. For only BG calcium measurement, 512 × 256 or 512 × 128 resolution image was acquired at 1 or 2 Hz.

Signal processing and data analysis

ROIs for PC, BG and MLI were carefully selected from high-resolution reference image by ZEN software. PC dendrite is brightly stained with OGB-1 and GCaMP6f is highly expressed that each dendrite was easily identified. BG was considered as SR101 positive regions during OGB-1 imaging (Nimmerjahn et al., 2009) and identified by signal induction by ES during GCaMP6f chronic imaging. The raw calcium signal traces were exported and analyzed using MATLAB (Mathwork). First, all traces were expressed as $\Delta F/F = (F - F_0)/F_0$, where F means mean fluorescence intensity of selected pixels at each frame and F_0 means the baseline intensity calculated as mean of the lowest 10 % of all values during each imaging session. Using high-pass filter for PC or low-pass filter for BG, signals between the two types of cells were successfully differentiated from the simultaneous Ca^{2+} imaging. After applying Gaussian smoothing to optimize the Ca^{2+} spike event detection, the dendritic calcium spikes of PC were effectively detected by setting the threshold as 5% for OGB-1 and 10 % for GCaMP6f increases compared to baseline intensity. To analyze the synchrony of PC dendritic Ca^{2+} spikes, Pearson's correlation coefficients between every pair of firing pattern across all ROIs were calculated and visualized as correlation matrix (Figure 8C). The 'network synchrony' was determined by averaging all Pearson's correlation values from every imaging session. In a similar manner, Pearson's correlation coefficients across all pairs of selected ROIs across all the imaging frames were presented as shown in Figure 8D.

Sensory stimulation

For LC neuron activation and NE release in cerebellum, electrical stimulations were delivered by a pair of percutaneous stimulating needles controlled by Pulse Master (WPI, FL). After inserting into fore- and hind-paw, one between first and second digits and another one between fourth and fifth digits, 0.2 ms square electrical pulses were given as 3 Hz with different intensities (0.1 – 20 mA) for indicated time. Normally 5-10 mA for 5-10 sec stimulation reliably induces prazosin-sensitive BG Ca^{2+} responses and PC Ca^{2+} spike suppression.

Cannulation and drug delivery

For local drug delivery into the lobule IV/V cerebellar vermis during chronic window imaging, guide cannula (Plastics One, VA) was installed on the lobule VI. Briefly, after removal of some part of muscles behind the cerebellum, a small hole was made (0.15-0.2 mm) by dental drill. The guide cannula was sharpened by obliquely beveling and injected 1-2 mm from skull at the angle of 35–40 degree from horizon in order that the tip of the internal cannula reaches right beneath (200 or 300 μm) of the cortex being imaged. During recovery, dummy cannula was inserted. Drug solution of 0.5 or 1 μl was injected using Pneumatic PicoPump (WPI, FL) through the inserted obliquely beveled internal cannula.

Drugs

For cortical drug application during two-photon Ca^{2+} imaging, 10 to 20 fold concentration compared to the ones for slice or *in vitro* experiments were used. 50 μM NBQX, 200 μM BAY 36-7620, 2 mM CPCCOEt, 100 μM prazosin, 25 μM TTX (Sigma) were used for cortical application. For hind limb anesthesia, 2% lidocaine-HCl (Huons) was injected. During cannula injection, 0.5 nmol of SR101 was injected. After an hour, 1, 1 and 50 nmol of prazosin, NPPB and NFA, respectively, were injected.

Statistical analysis

Graph plotting and statistical analysis was carried out by Origin software (Origin Lab). The hypothesis was tested by ANOVA with repeated measures followed by post hoc Bonferroni's test. Results were considered significant if *P* value is below 0.05. Asterisks denoted in the graphs indicate the statistical significance. * means *P* value < 0.05, ** < 0.01, *** < 0.001

RESULTS

Peripheral electrical stimulation (ES) reliably induces prazosin-sensitive Ca^{2+} transients in BG

Astrocytes in somatosensory cortex was shown to have Ca^{2+} transients in response to hind paw electrical stimulation (ES) (Bekar et al., 2008). Since it was dependent on the activity of locus coeruleus (LC) neurons which project axons throughout whole brain, I hypothesized that such a stimulation will activate LC and result in a release of norepinephrine (NE) to excite Bergman glia (BG), a major type of astrocyte in the cerebellum. To image BG intracellular Ca^{2+} level in response to ES, I utilized synthetic Ca^{2+} dye Oregon Green BAPTA-1/AM (OGB-1/AM) together with Sulfo-Rhodamine 101 (SR101) to specifically stain BG (Nimmerjahn et al., 2009) under two-photon microscopy in vermis of lobule IV/V. As shown in Fig. 1A, SR101 selectively stains BG that its Ca^{2+} transient was selectively identified by the regions for SR101 and OGB-1. In anesthetized mice, hind-paw ES (HPES) successfully triggers concerted Ca^{2+} excitation in cerebellar cortex (Figure 1B). The feature of the response corresponds to the flare response that is dependent on the motor activity, different from sparkle or burst in a previous study (Nimmerjahn et al., 2009). To characterize the optimal stimulation to maximize BG Ca^{2+} excitation, intensity, duration, frequency and inter-stimulus interval (ISI) were examined (Figure 1C). Finally, I find that stimulation of square pulses of 5 mA and 200 μs at 3 Hz for 5 sec induces saturated BG Ca^{2+} response which has refractory

periods of 60 sec ISI for the recovery of the initial response amplitude. These data suggest that peripheral stimulation directly activate Ca^{2+} responses in BG.

In ongoing experiments, such phenomenon was shown to be mediated by peripheral synaptic transmission as tested by hind limb (HL) injection of 10 μl of 2 % lidocaine-HCl (Figure 2A). Right HL lidocaine administration blocks BG Ca^{2+} response (BGCR) by right HPES but the response was still evoked by left HPES, which was totally abolished by left HL again. Centrally, application of TTX (25 μM) in the cerebellar cortex completely abrogates BG Ca^{2+} response by HPES (Figure 2B).

Next, since the present imaging area, cerebellar lobule IV/V vermis, is related to the sensation or movement of limbs and trunk, I tested whether the BG Ca^{2+} response is evoked in receptive field dependent manner or not. Surprisingly, not only HPES but also fore-paw, trunk and tail ES triggers BGCR (Figure 3A). Furthermore, hind-paw, fore-paw and trunk ES successfully induced Ca^{2+} response in astrocytes of the fore-limb region of somatosensory S1 cortex (Figure 3B). Such results support the involvement of LC afferents in HPES-induced BGCR since they project axons non-specifically to the whole brain area including cerebellar cortex.

Finally, to identify the specific signaling molecule involved in the BG Ca^{2+} response by HPES, I performed pharmacological experiments in the cerebellar cortex. BG express Ca^{2+} permeable ionotropic AMPA receptors to mediate kainite-induced Ca^{2+} excitation which was blocked by AMPA and NMDA receptor blocker (Muller et al., 1992). Also, PF brief burst stimulation was shown to induce BG Ca^{2+} response and it was completely blocked by

mGluR1 or P2Y receptor blocker. Hence, AMPA receptor blocker 2,3-dihydroxy-6-nitro-7-sulfamoyl-benzo[f]quinoxaline-2,3-dione (NBQX), NMDA receptor blocker (MK801) and mGluR1 non-competitive antagonist 7-(Hydroxyimino)cyclopropa[*b*]chromen-1a-carboxylate ethyl ester (CPCCOEt) or inverse agonist BAY 36-7620 were tested. As shown in Figure 4, although those drugs slightly attenuated the evoked responses, glutamate receptors do not appear as major mediators of the BGCR observed. In contrast, TTX application (25 μM) completely abolished the response. Also, treatment of P2Y receptor antagonist pyridoxal phosphate-6-azophenyl-2,4-disulfonic acid (PPADS) only causes partial effect on the ES-induced BGCR (Fig 4B). In a study in cerebellar slice, granule cell layer (GCL) stimulation induced Ca^{2+} transient in BG and it was not dependent on glutamate or P2Y receptor signaling but on α1-AR expressed in BG. To investigate whether α1-AR mediates HPES-induced BGCR, the α1-AR blocker prazosin (1 μM) was tested. As indicated in Figure 4B and E, prazosin completely blocked the evoked response. Taken together, it is concluded that peripheral electrical stimulation triggers a series of synaptic transmissions to activate LC neuron for NE release in brain areas including cerebellar cortex, resulting in BGCR.

Peripheral ES suppresses PC Ca^{2+} spike rate and amplitudes in cerebellum

Given that the peripheral ES induces NE release in cerebellar cortex as inferred by ES-triggered BGCR in anesthetized mice, one might ask whether the stimulation can modulate the activity of Purkinje cell (PC), the sole output of

cerebellum. So far several *in vivo* field recording and *in vitro* electrophysiological studies have investigated the effect of NE in the cerebellar circuitry. First of all, direct LC stimulation was shown to release NE in cerebellar cortex *in vivo* (Bickford-Wimer et al., 1991). Although a study indicated the dual effect of NE on PC, excitatory at low and inhibitory at high concentration of NE (Basile and Dunwiddie, 1984), majority of previous studies have investigated the inhibitory axis of NE on PC, reporting the suppression of PC activity through pre-synaptic or post-synaptic facilitation of GABAergic transmission (Cheun and Yeh, 1992; Moises et al., 1979; Parfitt et al., 1988; Saitow et al., 2000; Waterhouse et al., 1984).

Here, I asked whether PC activity is modulated by peripherally delivered ES. Recently, an ultra-sensitive version of genetically encoded Ca^{2+} indicator (GECI), GCaMP6, has paved a way for stable and successful detection of neuronal activity *in vivo* by two-photon microscopy (Chen et al., 2013). I used one of the GCaMP6 variants with fast kinetics, GCaMP6f, for the efficient detection of PC Ca^{2+} spikes. To exclusively express GCaMP6f in PC, AAV1-FLEX.GCaMP6f vector was introduced into the cerebellar cortex of pcp2-cre transgenic mice during chronic window preparation. Employing the CAG promoter and Cre-loxP system, GCaMP6f was successfully expressed in PC layer (PCL) and molecular layer (ML) ten days after chronic window preparation as shown in Figure 5. Though the expression levels among the cells were not homogeneous, PC Ca^{2+} spikes were successfully detected in most of the cells in a field of imaging (44 / 44 dendrites in Figure 6). For stabilization of the signals during possible motion artifacts and optimize spike detection,

Gaussian smoothing was applied. Since 10 % of changes of GCaMP6f mean intensity was shown to be above baseline, the threshold for Ca^{2+} spike detection was set as 10 % of ΔF/F. As indicated by previous observations, PC dendrites display synchronous activity of Ca^{2+} spikes reflecting the electrically coupled inferior olivary neuron activity (Ozden et al., 2009; Schultz et al., 2009). Average GCaMP6f spike rate and amplitude during resting state of anesthetized mice were 0.29 ± 0.011 Hz and 144.8 ± 8.1 % (ΔF/F). However, drastic suppression of PC Ca^{2+} spikes (0.15 ± 0.012 Hz, $P < 0.001$, Figure 6E) and amplitudes (53.8 ± 4.5 %, $P < 0.001$, Figure 6F) during 30 sec of HPES were observed. 30 sec right after the stimulation was halted, the frequency and amplitude were partially but significantly recovered (0.2 ± 0.011 Hz and 77.9 ± 6.6 %, $P = 0.02016$ and 0.02625, respectively, Figure 6E and F). Thus, peripheral ES resulted in dramatic reduction in frequency and amplitude PC in anesthetized mice.

ES-induced PC Ca^{2+} spike suppression coincides with BGCR in anesthetized mice

Recently, it is reported that glial cells actively contribute to modulate the neuronal activity and glial Ca^{2+} excitation is considered as an important feature in the neuroglia interaction (Kang et al., 1998; Lalo et al., 2014; Newman and Zahs, 1998; Poskanzer and Yuste, 2011; Torres et al., 2012). As the peripheral ES induced Ca^{2+} excitation of BG and the suppression of PC activity were observed, I asked whether the both phenomena occur at the same time. To corroborate this, simultaneous *in vivo* Ca^{2+} imaging of both cell types was

performed. Here, I report, for the first time, driven by ubiquitously active promoter (CAG) which is able to express transgenes in astrocytes (Lawlor et al., 2009), GCaMP6f is expressed in PC and BG as well (Figure 7A). Also, I infrequently detected GCaMP6f expression in MLIs (Figure 7A) but could not observed spontaneous or evoked Ca^{2+} transients during ES (data not shown). GCaMP6f expression was majorly seen in PC soma and dendrites but not in BG during resting state in anesthetized mice (N = 6 mice). However, BG showed concerted Ca^{2+} excitation during HPES together with suppression of PC Ca^{2+} spikes (Figure 7B and C). It can be thought that the basal Ca^{2+} level in BG is too low to be detected by GCaMP6 but evoked response is successfully observed. In contrast, due to high basal calcium level, PC display bright signals of GCaMP6. Still, the signals of BG were not well discriminated from that of PC after manually selecting ROIs since they locate very close to each other and BGCR elicits Ca^{2+} elevation in the field outside the fine fibers of the projections (Nimmerjahn et al., 2009). Hence, by applying high-pass filter for the PC signal and low-pass filter for the BG signal, each signal was successfully separated (Figure 7D and E). After applying Gaussian smoothing, pure PC and BG Ca^{2+} transient traces were shown in Figure 7D and E. Thus, in this set of experiment, PC Ca^{2+} spike suppression was shown to well coincide with BGCR, possibly suggesting the interaction between the both cell types during ES-evoked NE release.

Awake GCaMP6f chronic imaging revealed dissected kinetics of PC, BG and MLI in response to NE release by arousal

Recently, it is reported that the activity of astrocytes is inhibited by general anesthesia (Nimmerjahn et al., 2009; Thrane et al., 2012) and their functions are different between sleep/wake and awake state (Xie et al., 2013). Hence, the need for corroboration of the present results in awake behaving mice is evident. The peripheral ES-induced BGCR appears to be "flare response" that was recorded during the activation of motor behavior in a previous report (Nimmerjahn et al., 2009). More recently, this type of Ca^{2+} response was shown to be associated with the locomotion-triggered arousal and depend on α1-AR activation (Paukert et al., 2014). Here, I hypothesized that BGCR may coincide with PC Ca^{2+} spike suppression during arousal in awake behaving mice. First of all, the dendritic Ca^{2+} spike activity and its network during awake resting state was characterized. The 34 ROIs were selected from 16 Hz spontaneous Ca^{2+} imaging movie (Figure 8A). The average frequency and amplitude appeared to be 0.97 ± 0.22 Hz and 54.0 ± 11.4 % (ΔF/F), respectively (Figure 8B). Also, one of the prominent feature of the dendritic Ca^{2+} spike network is the synchronous activity between dendrites, which is known to be involved in exact timing of the motor execution (De Gruijl et al., 2014). The synchrony analysis indicates moderate co-activation across the dendrites imaged, the network synchrony value being 0.267 (Figure 8C). Also, to characterize whether the correlation changes across time during resting state, Pearson's correlation was calculated between every pair of event patterns across all frames. As presented in the time correlation matrix, the correlation shape looks even, suggesting that the activity network does not dramatically change over time (Figure 8D). The synchrony was also indicted by the intensity profile

matrix and the event detection and cumulative plots (Figure 8F). Based on the result of PC dendritic Ca^{2+} spike characterization, other experimental condition was tested.

Next, to determine whether BGCR and PC suppression coincide in awake behaving mice, I performed PC-BG simultaneous Ca^{2+} imaging in awake mice that is experiencing the arousal. Due to the stress from head-restraint, mice sometime showed escaping behavior which definitely includes the locomotive activation, termed as 'spontaneous arousal'. Or I gave arousal stimuli by pulling the tail or touching the whisker, termed as 'evoked arousal'. In such contexts of arousal, Ca^{2+} imaging of PC and BG was performed. As shown in Figure 9, PC dendritic Ca^{2+} spikes show synchronous activity during resting state. When they start escaping behavior in response to arousal stimuli, they exhibit sudden co-activations of PC Ca^{2+} spikes, directly followed by Ca^{2+} excitations of BG and MLI (Figure 9A, B and C). The dendritic Ca^{2+} spikes are suppressed after arousal stimuli and the time appears to be several seconds after arousal stimuli. The phase during which PC activity is suppressed after arousal is estimated to be during 10 seconds. I compared the event frequency and amplitude during first 20 sec (phase 1; resting phase), 10 sec after arousal stimuli (phase 2; inhibition phase), and last 20 sec (phase 3; recovery phase) from 60 sec recording and found that arousal stimuli induces significant decrease of event rates ($P < 0.001$, Phase 1 vs 2) and amplitudes ($P = 0.02$, Phase 1 vs 2) and they were moderately recovered in phase 3 (Figure 9E). Collectively, BGCR was shown to coincides with PC activity suppression also coincides in awake behaving mice.

Cerebellar vermis α1-Adrenoreceptor blockade causes massive synchrony and tremendously increased amplitudes of PC Ca^{2+} spike

To investigate the role of BGCR in modulation of PC activity during arousal, pharmacological approach was used by utilizing cannulation in chronic window imaging. During preparation of chronic window for GCaMP6 imaging, a guide cannula was installed so that the tip of the cannula, penetrating from the occipital bone of posterior lobules, reaches right below of the cerebellar cortex that is being imaged (Figure 10A). To ensure the successful delivery of the drugs and stain BG process as well, 5 nmol SR101 was co-injected. 90 min after injection, BG soma around PCL and processes in ML was clearly identified (Figure 10B). Utilizing such system, prazosin was tested whether the α1-adrenoreceptor blockade affect the PC activity during arousal. Surprisingly, 1 nmol prazosin injection resulted in impaired locomotive activity and rarely showed spontaneous arousal (data not shown). This is consistent with a study suggesting that α1-AR blocker treatment in cerebellar vermis diminished behavioral activation and increased the time of immobilization in a novel cage (Stone et al., 2004). Mice also showed behavior of anxiety such as leaning on the wall (Figure 11F). During imaging, prazosin injection induced abnormally high synchrony network (averaged Pearson's correlation = 0.93, Figure 11D) and amplitudes of PC Ca^{2+} activity (198.55 ± 46.5 % (ΔF/F) from 36 dendrites, Figure 11B and C). Next, when arousal stimuli was given, BGCR was not detected (data not shown) but the amplitudes of evoked PC Ca^{2+} response were even higher than spontaneous ones (Figure 12). Taken together, α1-AR

inhibition causes aberrant network activity of PC and these results emphasize the contribution of BG and their α1-AR activity in maintaining the Ca^{2+} network and regulating the magnitudes of amplitudes.

Prazosin-induced massive synchrony of PC dendritic Ca^{2+} signal spans through whole cerebellar vermis

The PC dendritic spike synchrony is previously known to fall off within 100 or 200 μm and the domain of synchronized activity is called 'microbands' or 'microzone' (Ozden et al., 2009; Schultz et al., 2009). To determine the length of the altered massive synchrony PC dendritic Ca^{2+} activity induced by prazosin, I performed the Ca^{2+} imaging of PC dendrites using lens with low magnification (5×) to cover much wider region. Compared to 20× lens which visualizes 500 μm mediolaterally, 5× lens enables to image 1700 μm length. From the imaging field, 10 ROIs were selected at 160~170 μm interval and the traces were depicted (Figure 13A and C). Interestingly, the massive synchrony within mediolateral 1700 μm is obvious as seen from the traces (Figure 13A below). The changes of Ca^{2+} spike amplitudes was clearly presented from field image of each indicated time (Figure 13C). Finally, average synchrony was calculated to be 0.934 (Figure 13B), similar with the 20× lens imaging result (Figure 11). These results indicate that α1-AR is a major contributor in supporting proper synchrony of PC dendritic Ca^{2+} spike network and response amplitudes. Thus, it can be inferred that the α1-AR activation in BG during arousal would serve as a pathway that relates with PC suppression.

β-adrenoreceptor Blockade by Propranolol Does Not Severely Affect PC Network Activity

Since the β-ARs are abundantly expressed in cerebellum and localize in PC and MLI, enhancing GABA transmission in response to NE (Saitow et al., 2000), whether their activations contribute to arousal-induced PC suppression should be answered. To test this possibility, the pan-βAR blocker propranolol was injected into the cerebellar vermis and PC activity was monitored. The frequency and amplitudes were moderately increased (1.15 ± 0.46 Hz and 52.68 ± 8.16 % (ΔF/F), respectively from 43 ROIs, Figure 14B). It would be due to the result of disinhibition by the blockade of βAR-mediated IPSC augmentation. Also, the network synchrony was similar with that of normal condition (averaged Pearson's correlation = 0.209, Figure 14C). Taken together, it can be suggested that the effect of β-AR in regulating the PC activity and its network is limited to moderate enhancement of GABAergic transmission.

Glial GABA channel Best1 blockade by NPPB in cerebellar vermis causes massive synchrony and tremendously increased amplitudes of PC Ca^{2+} spike activity

Next questions is about what consequences of α1-AR activation in BG are involved in PC suppression during arousal. Accumulating evidence indicate that interactions between neurons and glia comprise of gliotransmission that functionally affects the neuronal excitability (Kang et al., 1998; Torres et al., 2012; Wang et al., 2012). A recent finding suggest that the release of GABA

from BG mediates tonic inhibition in cerebellum by direct permeation through Bestrophin1 channel (Lee et al., 2010). Also, it was shown that BG phasically release GABA in a Ca^{2+}-dependent manner in response to certain types of agonists such as protease activated receptor (PAR) expressed on BG (Yoon et al., 2014). Furthermore, it has been suggested that low amount of ambient GABA can activate extrasynaptic $GABA_A$ receptor to yield tonic conductance (Farrant and Nusser, 2005). Hence, I hypothesized that BG would release GABA and strongly contribute to the suppression of PC activity during arousal. To test this possibility, the Best1 blocker 5-nitro-2-(3-phenylpropylamino)-benzoate (NPPB) was injected into the cerebellar lobule V/VI vermis. Remarkably, the effect of NPPB on PC activity network was similar with that of prazosin (Figure 15). In the presence of NPPB, PC dendritic Ca^{2+} network synchrony appeared abnormally high (averaged Pearson's correlation = 0.964, Figure 15C). The amplitudes of Ca^{2+} spikes were also aberrantly increased (210.75 ± 54.34 % (ΔF/F) from 39 PC dendrites, Figure 14B). The amplitudes in response to arousal stimuli were much higher than those of the spontaneous ones (445.2 ± 0.95 % (ΔF/F) from 39 PC dendrites, Figure 15A). Behaviorally, mice showed impaired locomotive activity and motor coordination (data not shown). In sum, Best1 blockade in cerebellar vermis induces massive synchrony in PC dendritic Ca^{2+} activities with abnormally increased amplitudes and strongly suggesting the positive relationship between α1-AR activation and Best1-mediated GABA release by BG.

To corroborate the prominent role of Best1 in regulating PC activity suppression, another blocker Niflumic acid (NFA) was tested in the same

experimental setting. The mice injected with NFA in cerebellar vermis V/VI showed impaired locomotive activity and motor coordination. Outstandingly, they exhibited dystonic behavior such as abnormal posture, writhing behavior and stretching the hind limb (Figure 17A). Similarly with NPPB, 50 nmol NFA injection increased the network synchrony of PC dendritic Ca^{2+} activity (averaged Pearson's correlation = 0.57, Figure 16C). The amplitudes were not changed compared with normal condition from longitudinal study (58.45 ± 17.2 % (ΔF/F), Figure 16B, Normal condition: 54.0 ± 11.4 % (ΔF/F) from Figure 8B). Remarkably, they displayed dystonic posture after the arousal stimuli was given as snapshots of indicated time points from the imaging were shown in Figure 17B. More interestingly, the PC Ca^{2+} burst activity occurs when the dystonic posture is presented (Figure 17C). Also, the time presented with abnormal body posture corresponds with when the PC activity is suppressed in response to arousal stimuli in the normal condition (Figure 9E). Hence, these results strongly implicate the function of Best1 as a major contributor of proper regulation of the network synchrony and inhibition of PC activity. In other words, it can be suggested that the impairment of Best1 activity can cause aberrant synchronous burst activity of PC and produce unusually elevated output to deep cerebellar nuclei (DCN) which in turn will relay such abnormal outputs to other motor areas including motor cortex or basal ganglia, finally inducing the dystonia (Figure 18). This explanation is supported by recent findings indicating the prominent role of cerebellum in pathophysiology of motor disease such as dystonia (Calderon et al., 2011; Filip et al., 2013). Collectively, it can be suggested that the modulation of a single

cell type, glia, and more specifically a single molecule of BG, GABA channel Best1, can critically affect the PC activity network or the output and consequently cerebellum-dependent motor coordination (Figure 18).

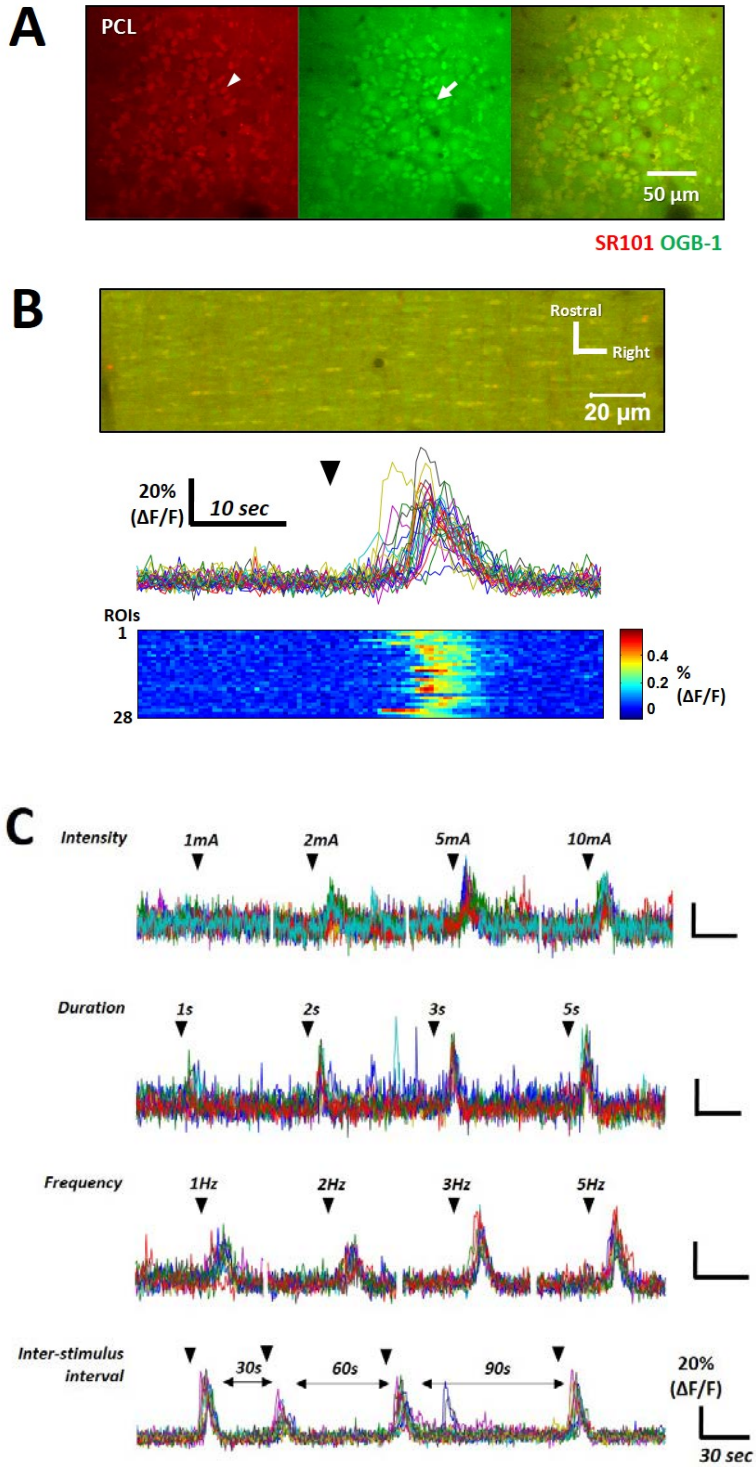
A
PCL
50 µm
SR101 OGB-1
B
Rostral
Right
20 µm
20%
(ΔF/F)
10 sec
ROIs
1
28
0.4
0.2
0
%
(ΔF/F)
C
Intensity
1mA
2mA
5mA
10mA
Duration
1s
2s
3s
5s
Frequency
1Hz
2Hz
3Hz
5Hz
Inter-stimulus
interval
30s
60s
90s
20%
(ΔF/F)
30 sec

Figure 1. Peripheral Electrical Stimulation (ES) induces Ca^{2+} responses in Bergmann Glia (BG).

(A) A high resolution reference image of OGB-1/AM staining in cerebellar cortex Purkinje cell layer (PCL) lobule IV/V. SR101, OGB-1/AM and merged image, left to right. A white arrow head and an arrow indicate soma of Bergmann glia (BG) and Purkinje cell (PC) in PCL, respectively. Scale bar was indicated. (B) A high resolution reference image of OGB-1/SR101 staining from molecular layer (top). SR101 (Red) and OGB-1 (green) double positive regions indicate BG processes stained with OGB-1. Normalized ΔF/F traces of OGB intensity traces and intensity profile matrix of 28 selected ROIs of BG processes (bottom). Black arrow head indicates 5 mA hind-paw electrical stimulation (HPES) for 5 sec. The right panel of the intensity matrix represents the scale bar of intensity changes compared to the baseline (presented as % ΔF/F). (C) BG Ca^{2+} trace (ΔF/F) data from 10 selected ROIs from testing optimal intensity, duration, frequency and inter-stimulus interval (ISI). 200 μs square pulses of 5 mA during 5 sec at 3Hz stimulation condition was tested for indicated intensity, duration, frequency and ISI. Scale bar for percent change of ΔF/F and the time were indicated on the right side.

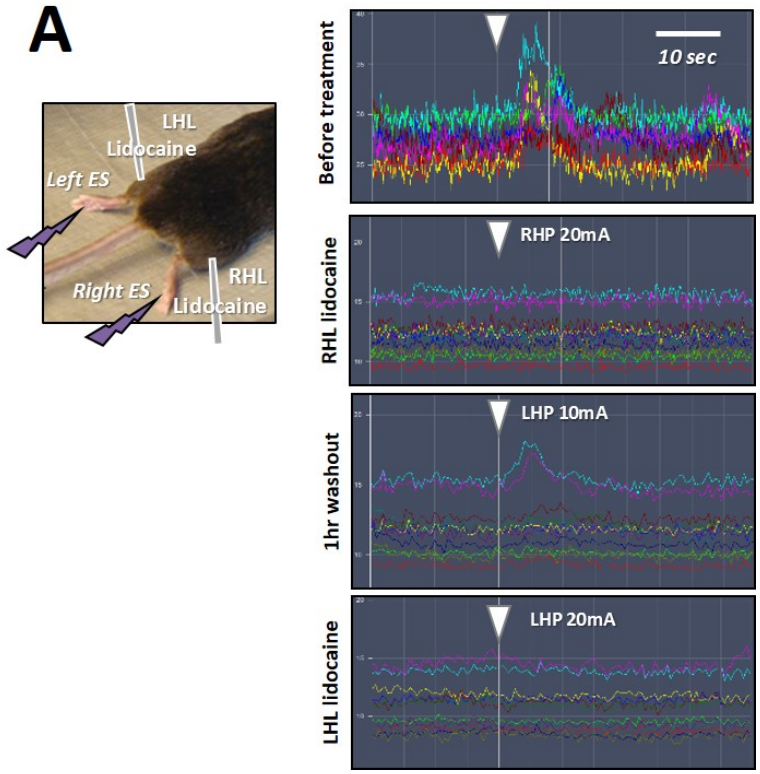
A
LHL
Lidocaine
Left ES
Right ES
RHL
Lidocaine
Before treatment
10 sec
RHL lidocaine
RHP 20mA
1hr washout
LHP 10mA
LHL lidocaine
LHP 20mA

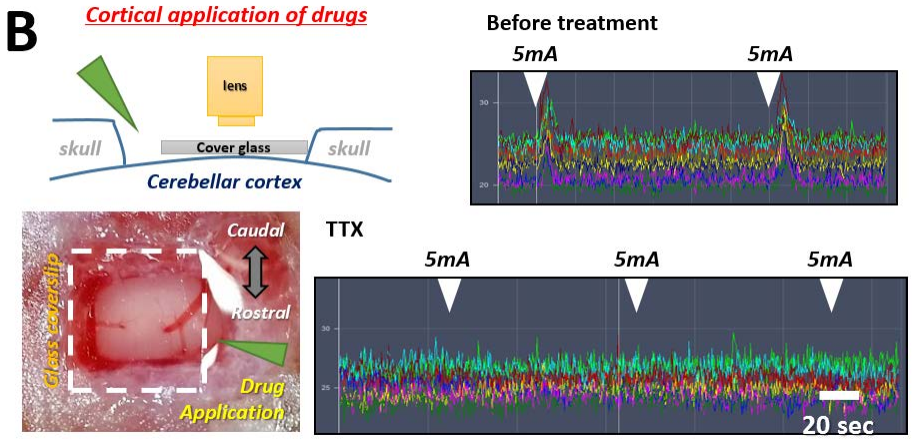
B
Cortical application of drugs
lens
skull
Cover glass
skull
Cerebellar cortex
Caudal
Rostral
Glass coverslip
Drug
Application
Before treatment
5mA
5mA
TTX
5mA
5mA
5mA
20 sec

Figure 2. HPES-induced BGCR is mediated by peripheral and central synaptic transmission

(A) (Left) Diagram representing the locations of electrodes (purple) and drug injections (gray). (Right) BG Ca^{2+} traces in response to HPES of 5 mA of intensities otherwise indicated before treatment, after right hind-limb (RHL) lidocaine injection, after 1 hour washout and after left hind-limb (LHL) lidocaine injection. (B) (Left and below) Diagram for imaging area during cortical application of the drug. (Right and below) BG Ca^{2+} traces in response to HPES of 5 mA before and after TTX 25μM 15min treatment. White arrow heads represent onset of HPES of 10 sec.

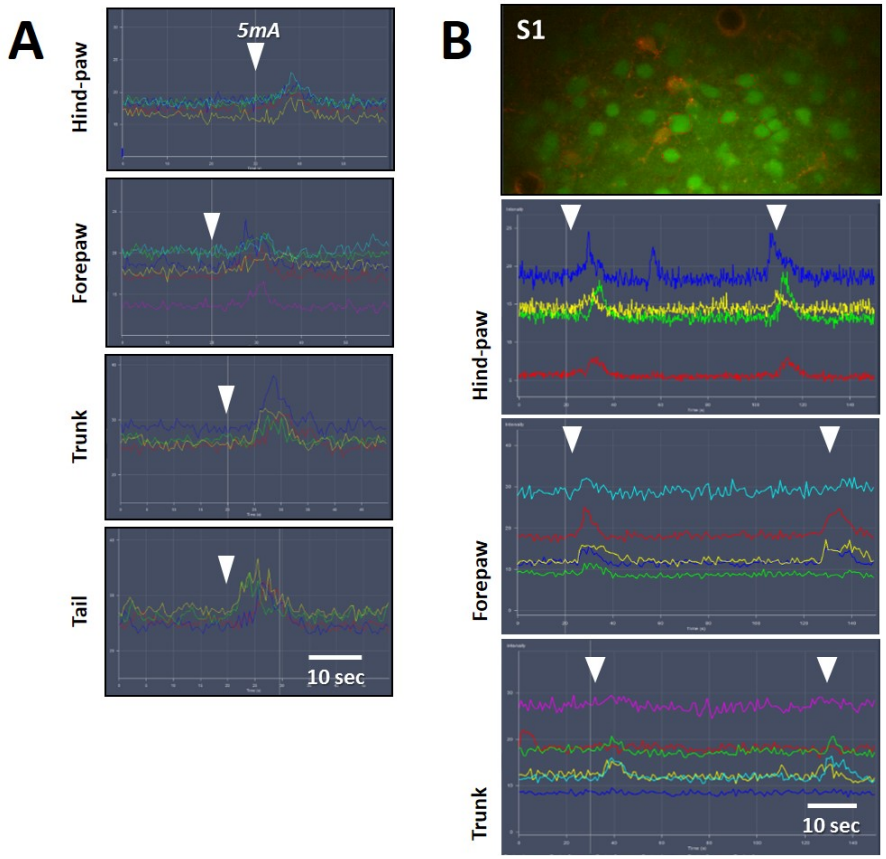

Figure 3. Glial Ca^{2+} responses in broad brain area by stimulations at broad sites.

(A) Cerebellar BG Ca^{2+} traces in response to HPES of 5 mA at hind-paw, forepaw, trunk and tail. (B) (Top) A high resolution reference image in S1 sommatosensory cortex fore-limb region during OGB-1AM Ca^{2+} imaging. Cells stained with SR101 (Red) represent astrocytes. BG Ca^{2+} traces in response to HPES at hind-paw, forepaw, and trunk. White arrow heads indicate onset of HPES.

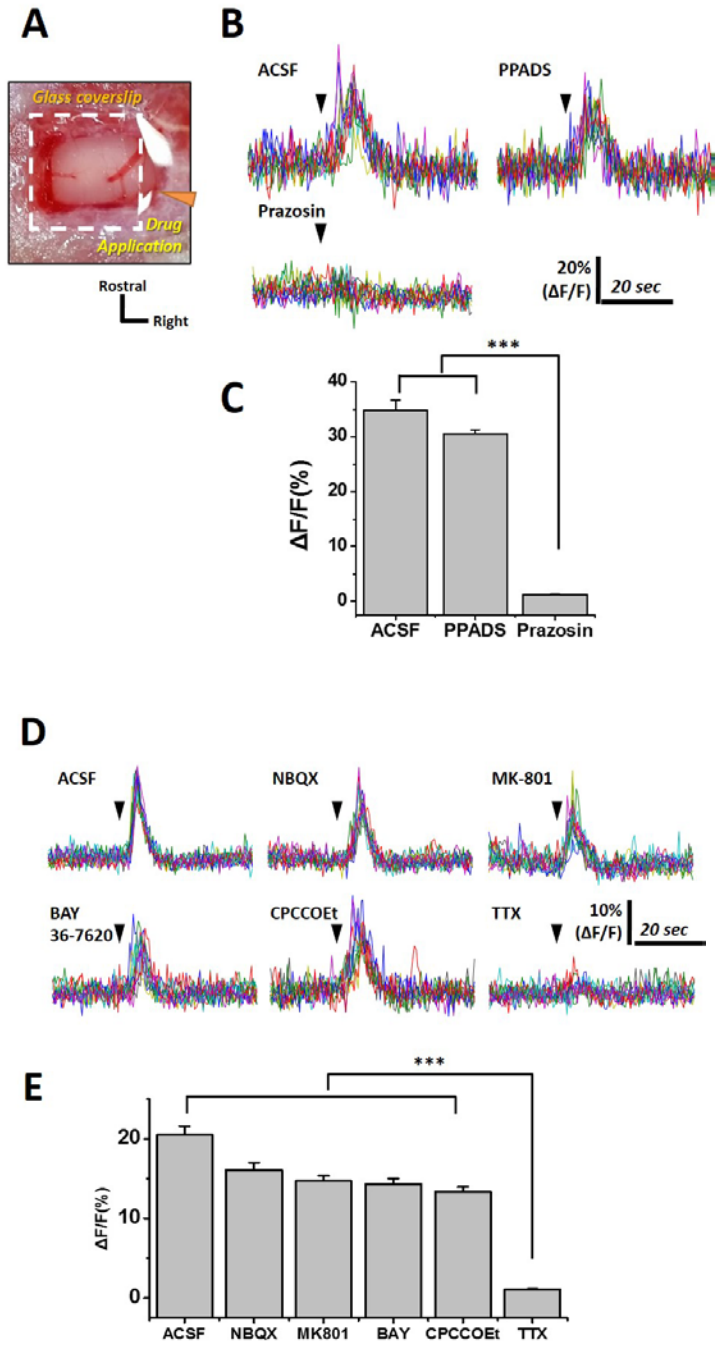
A
Glass coverslip
Drug Application
Rostral
Right
B
ACSF
PPADS
Prazosin
20%
(ΔF/F)
20 sec
C
***
ΔF/F(%)
40
30
20
10
0
ACSF
PPADS
Prazosin
D
ACSF
NBQX
MK-801
BAY
36-7620
CPCCOEt
TTX
10%
(ΔF/F)
20 sec
E
***
ΔF/F(%)
20
10
0
ACSF
NBQX
MK801
BAY
CPCCOEt
TTX

Figure 4. HPES-induced BG Ca^{2+} response is exclusively mediated by α1-AR activation.

(A) The image of cerebellar cortex being imaged during cortical application of the drugs. The size of the square hole of the cranial window corresponds to 1.2 X 2.2 mm. (B, D) Normalized ΔF/F traces of BG Ca^{2+} level during cortical bath application of ACSF, 1 mM PPADS, 100 μM prazosin (B), 50 μM NBQX, 200 μM BAY 36-7620, 2 mM CPCCOEt and 25 μM TTX (C). Black arrow heads indicate the onset of 5 mA HPES for 5 sec. (C and E) Normalized ΔF/F amplitudes changes in response to HPES (5 mA) with cortical applications indicated drug (N = 3 mice each). Statistics tested by ANOVA with repeated measures with post hoc Bonferroni's test. *** indicates statistical significance at P value <0.001.

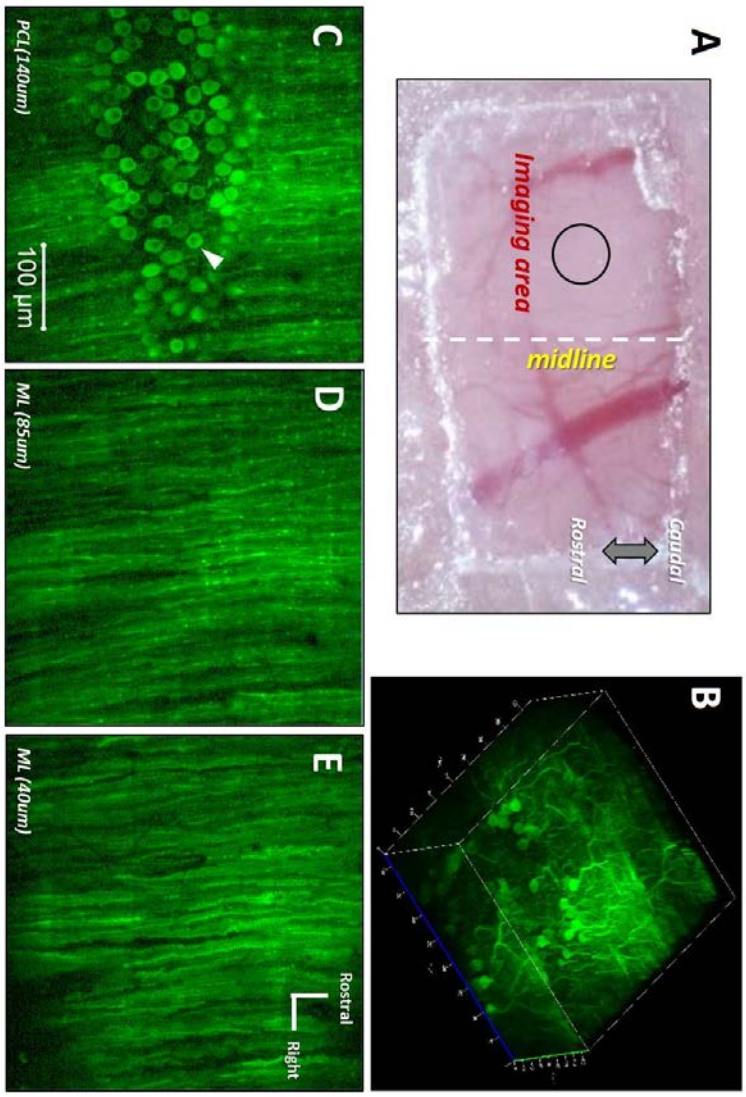

Figure 5. Specific expression of GCamP6f in Purkinje cell using pcp2-cre TG mouse utilizing cre-lox system.

(A) An image of chronic window located on cerebellar vermis lobule V and VI of mice at post operation (PO) day 14. The midline, the imaging area and the direction were indicated. (B) A 3D projection image of GCaMP6f specifically expressed PC obtained by two-photon microscopy in pcp2-cre transgenic mouse cerebellar cortex (C, D and E) Representative images of GCaM6f in 140 (PC layer), 85 and 40 μm (ML) from dura. An arrow head indicates soma of PC. PC dendrites are parasagittaly aligned in ML (D and E).

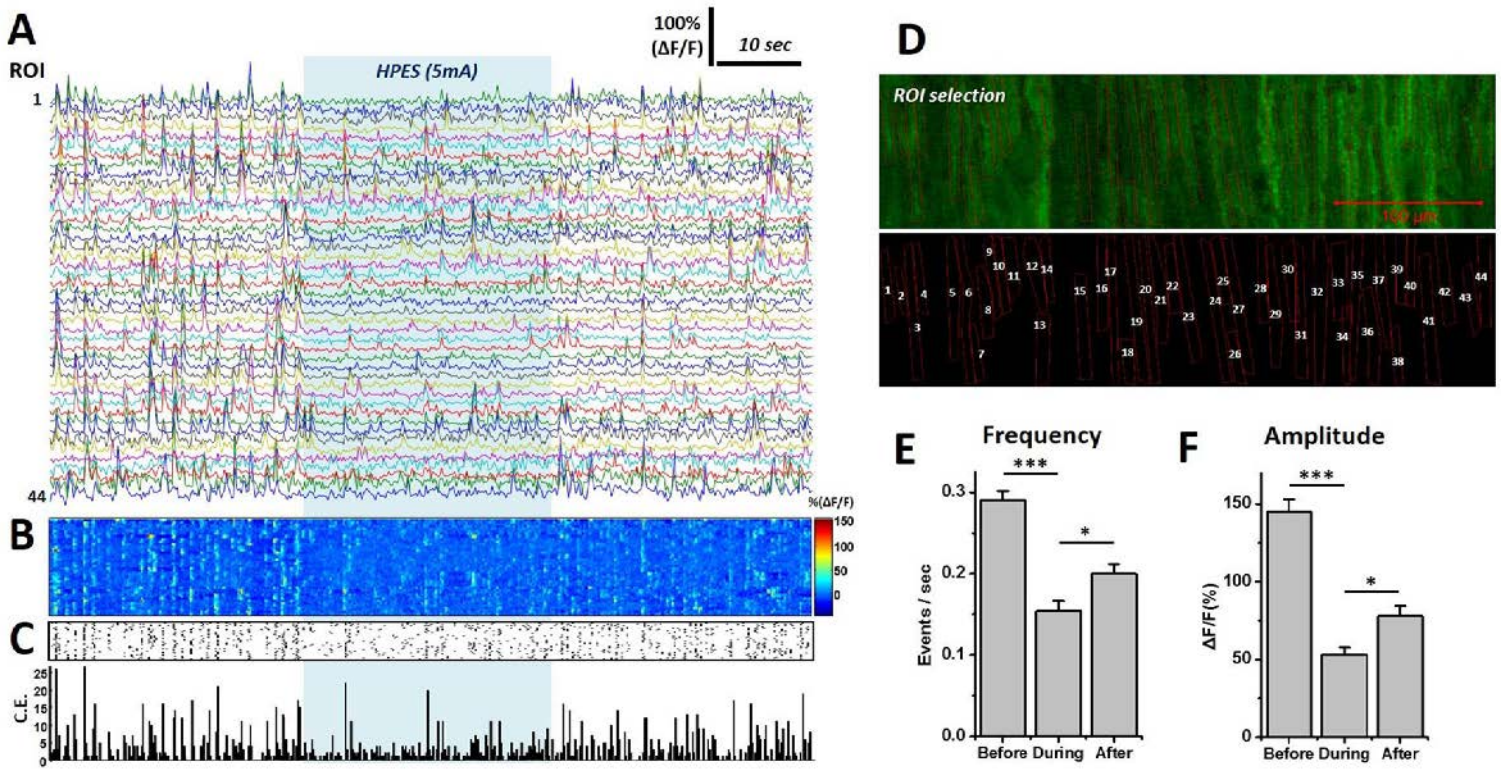
A
ROI
1
44
100%
(ΔF/F)
10 sec
HPES (5mA)
B
%(ΔF/F)
150
100
50
0
C
C.E.
25
20
15
10
5
0
D
ROI selection
100 μm
E
Frequency
***
*
Events / sec
0.3
0.2
0.1
0.0
Before During After
F
Amplitude
***
*
ΔF/F(%)
150
100
50
0
Before During After

Figure 6. Peripheral noxious ES drastically down-regulate PC Ca^{2+} spike rates and amplitudes in anesthetized mice.

(A) Normalized ΔF/F traces from 44 ROIs of PC dendrites. HPES of 5 mA for 30 seconds during the middle of the whole 90 sec imaging (8Hz frame rate) was indicated by a box with light blue. The suppression of PC dendritic Ca^{2+} events are apparent. (B) Intensity profile matrix of 44 ROIs reflecting frequency and amplitudes at each frame. (C) Event rate raster plot (top) and cumulative event number plot (C. E., bottom) indicating the event frequency and co-activation across all ROIs. (D) A high resolution reference image for the imaging field (top) and an image showing selection of 44 ROIs with red boarders (bottom). (E and F) Comparison of mean frequencies (events / sec, Hz) and the amplitudes (% changes in ΔF/F of each dendrite) before, during and after HPES. Data are presented as Hz or ΔF/F (%) ± SD. Statistical significance was tested by ANOVA with post hoc Bonferroni's test. * and *** indicate statistical significance at P value < 0.05 and <0.001, respectively.

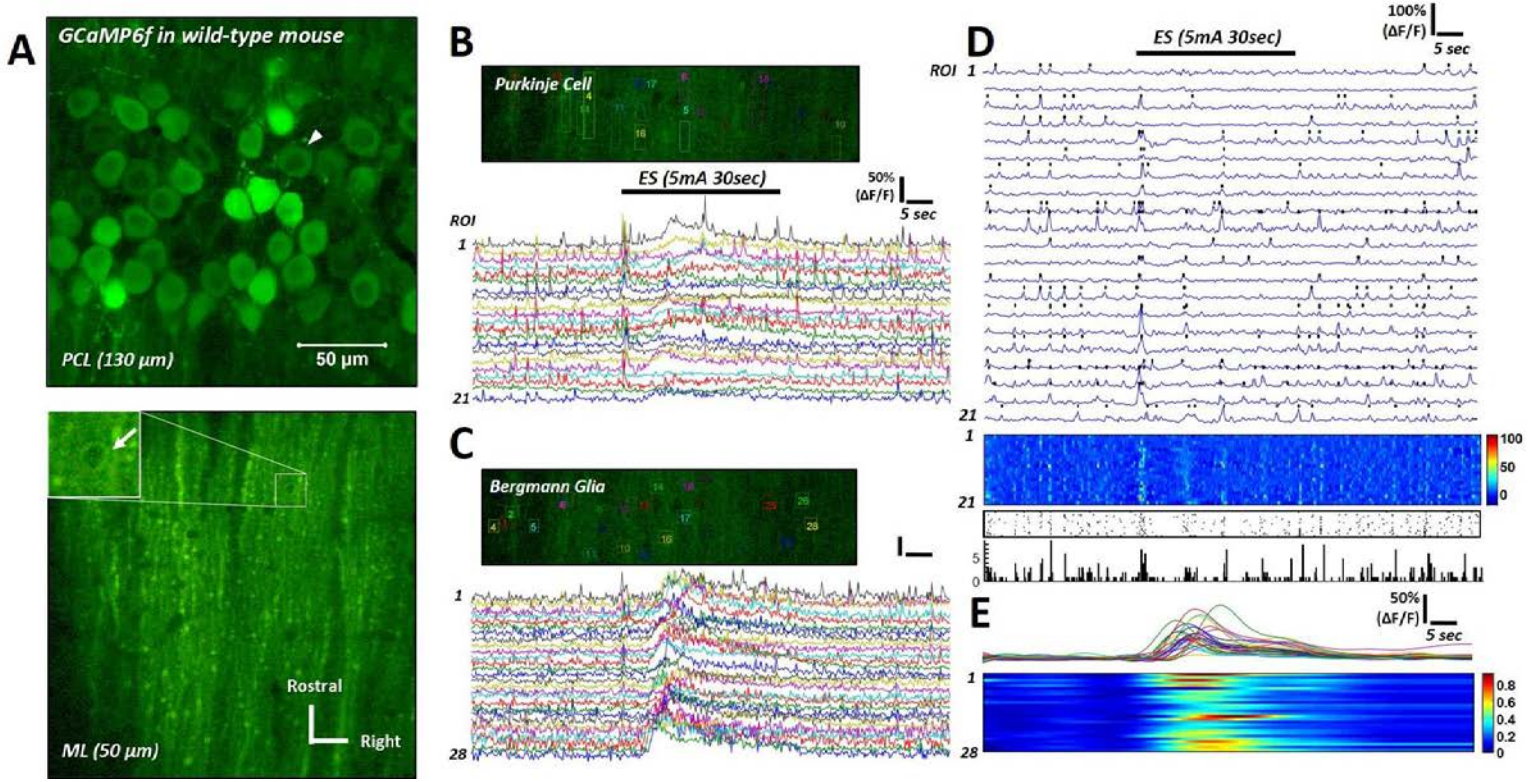
A
GCaMP6f in wild-type mouse
PCL (130 μm)
50 μm
ML (50 μm)
Rostral
Right
B
Purkinje Cell
ES (5mA 30sec)
50%
(ΔF/F)
5 sec
ROI
1
21
C
Bergmann Glia
1
28
D
ES (5mA 30sec)
100%
(ΔF/F)
5 sec
ROI
1
21
100
50
0
5
0
E
50%
(ΔF/F)
5 sec
1
28
0.8
0.6
0.4
0.2
0

Figure 7. The separation of PC dendritic Ca^{2+} activity and BGCR from multi-cell simultaneous calcium imaging: Coincidence of PC suppression and BGCR during peripheral noxious ES in anesthetized mice.

(A) Images of GCaMP6f from two-photon microscopy in wild-type mouse cerebellar cortex virally expressed with GCaMP6f in PC layer (130 μm) and ML (50μm). A white arrow head indicates soma of PC. The enlarged small white box in the bottom image indicates the expression of GCaMP6 in molecular layer interneuron (MLI) and a white arrow represents MLI. (B) 21 ROIs of PC dendrites selected from the imaging field (top) and normalized ΔF/F traces from them with signal processing (bottom). HPES of 5 mA for 30 seconds was indicated with black bar. (C) 28 ROIs of BG processes with intensity changes for more than several seconds were selected from the imaging field (Top) and normalized ΔF/F traces were shown (bottom). (B and C) The signal contamination is present between PC dendrites and BG processes selected. (D) Traces of PC dendritic Ca^{2+} level after signal processing of high-pass filtering and Gaussian smoothing, resulting in pure PC Ca^{2+} spike from the PC-BG simultaneous Ca^{2+} imaging (top). Intensity profile matrix of the 21 ROIs reflecting frequencies and amplitudes at each frame (intermediate). Event rate raster plot and cumulative event number plot (C. E.) representing the frequency and synchrony of Ca^{2+} spikes (below). (E) BG Ca^{2+} traces after signal processing of low-pass filtering and Gaussian smoothing (top) and intensity profile of selected 28 ROIs (bottom).

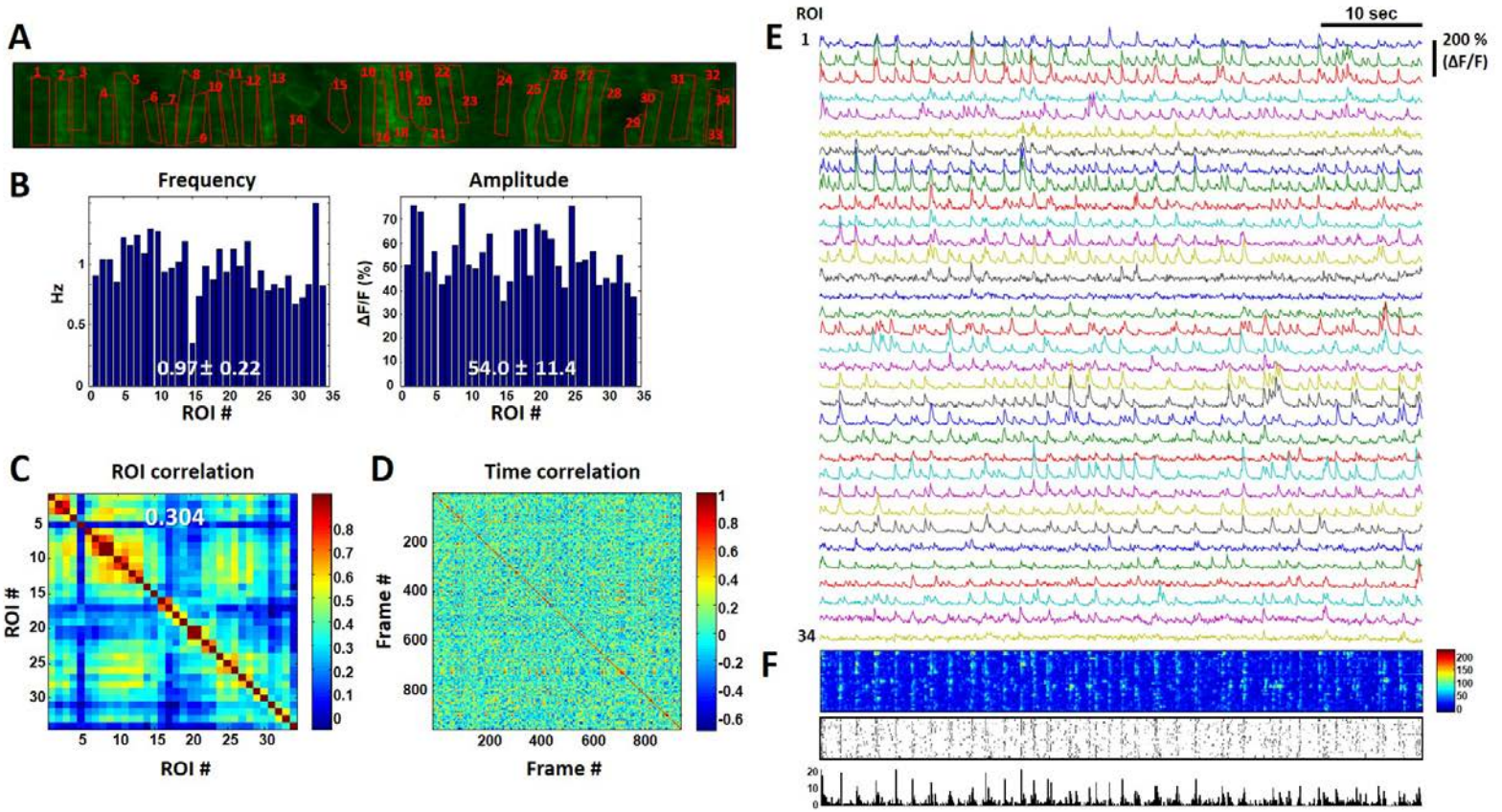
A
B
Frequency
Amplitude
Hz
ΔF/F (%)
0.97 ± 0.22
54.0 ± 11.4
ROI #
ROI #
C
ROI correlation
0.304
ROI #
ROI #
D
Time correlation
Frame #
Frame #
E
ROI
1
34
10 sec
200 %
(ΔF/F)
F

Figure 8. Characterization of PC dendritic Ca^{2+} spike in awake mice.
(A) An image showing selection of 34 ROIs (Red border) from a high resolution image of virally transduced GCaMP6f PC dendrites from PO day 14 wild-type mice. (B) The frequencies and amplitudes of selected ROIs were presented as Hz and ΔF/F (%), the average values presented inside each graph. (C) Synchrony matrix drawn from Pearson's correlation value of each pair across all ROIs. X- and Y-axis indicate ROI number (#). The Pearson's correlation values rages from -1 to 1. -1, 0 and 1 indicate perfect negative correlation, no correlation and perfect positive correlation, respectively. The average of all the Pearson's correlation values from all pairs across all ROIs were depicted inside the box. (D) Time correlation matrix which shows the Pearson's correlation values from event patterns of every pair of imaging frames. X- and Y-axis indicate frame number (#). (E) GCaMP6f traces from selected ROIs during 60 sec. (F) The intensity profile of the PC Ca^{2+} traces reflecting events and their strengths (top). Event cumulative (E.C.) plots (middle) and co-activation plot (down).

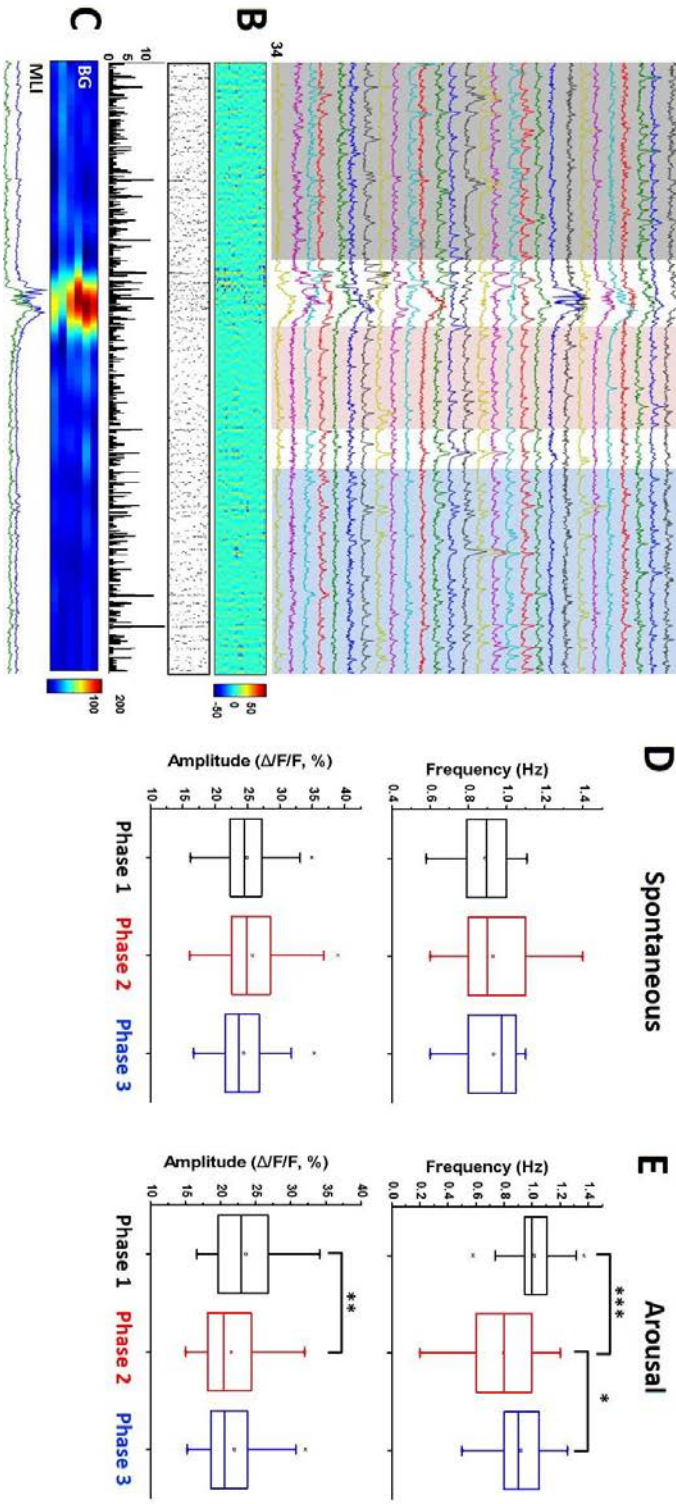
A
Evoked Arousal
Phase 1
Phase 2
Phase 3
10 sec
PC
200 %
(ΔF/F)
B
C
BG
MLI
D
Spontaneous
Frequency (Hz)
Amplitude (Δ/F/F, %)
Phase 1
Phase 2
Phase 3
E
Arousal
***
*
**

Figure 9. Arousal induced BGCR and PC suppression in awake behaving mice.

(A) Ca^{2+} signal traces from selected 34 ROIs during 60 sec. Arousal stimuli was given at 20 sec (the red arrow). Phase1, 2 and 3 indicate resting, inhibition and recovery phase. (B) The intensity profile of the PC Ca^{2+} signals reflecting events and the strengths (top). Event cumulative (E.C.) plots (middle) and co-activation plot (down). (C) Normalized BG intensity profile after signal processing of low pass filtering and Gaussian smoothing (top). Ca^{2+} traces from two MLIs. (D and E) Box plot graphs comparing frequencies and amplitudes during pahse1, 2 and 3 of Ca^{2+} imaging at resting (D) and at the arousal context (E). The data were presented as Hz for frequency and $\Delta F/F$ (%) for amplitudes. Statistical significance was tested by ANOVA with post hoc Bonferroni's test. *, ** and *** indicate statistical significance at P value < 0.05, 0.01 and 0.001, respectively.

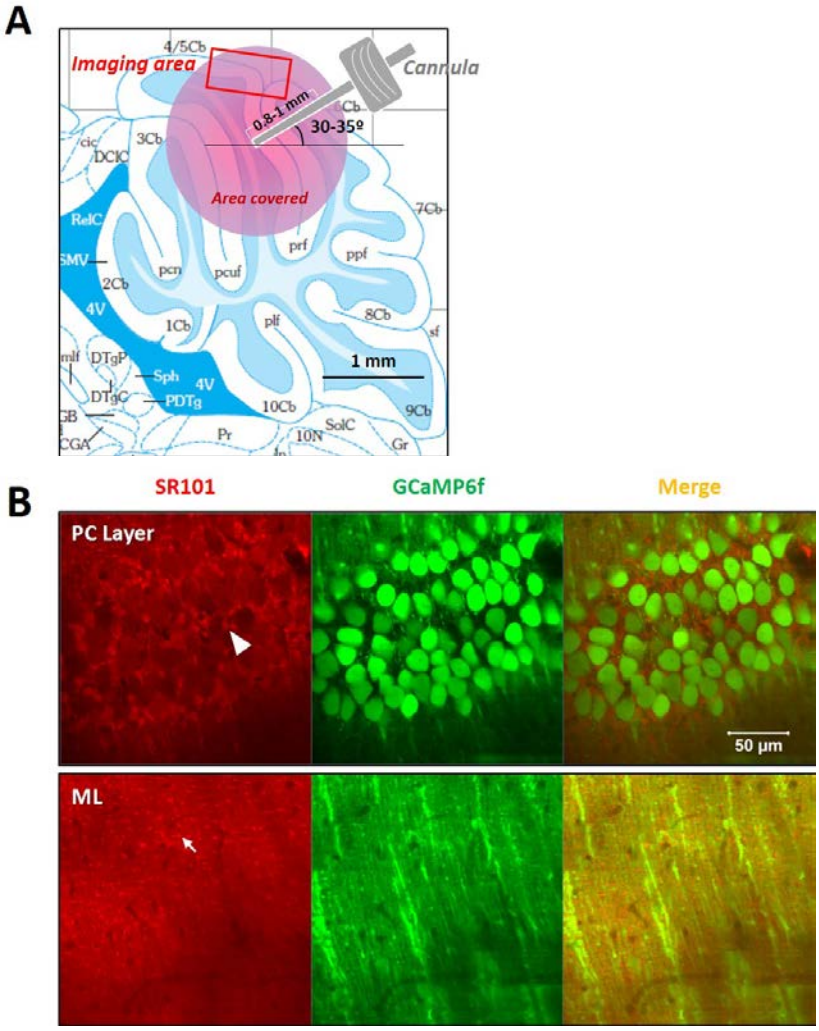

Figure 10. The drug delivery system for chronic window imaging guided by cannula.

(A) A diagram illustrating the cannula setup location in cerebellar vermis and drug delivery condition. The cannula is inserted into anterior region of lobule six vermis with 30 to 35º from horizontal line. Total 1 µl injection of drug will result in 1 - 1.5 mm diffusion from the injection site. (B) Images taken from two-photon microscopy after 90 min of SR101 injection into GCaMP6f expressed cerebellum. SR101, GCaMP6 and Merge images were presented left to right. A white arrow head and a white arrow indicates BG soma and process successfully stained with SR101.

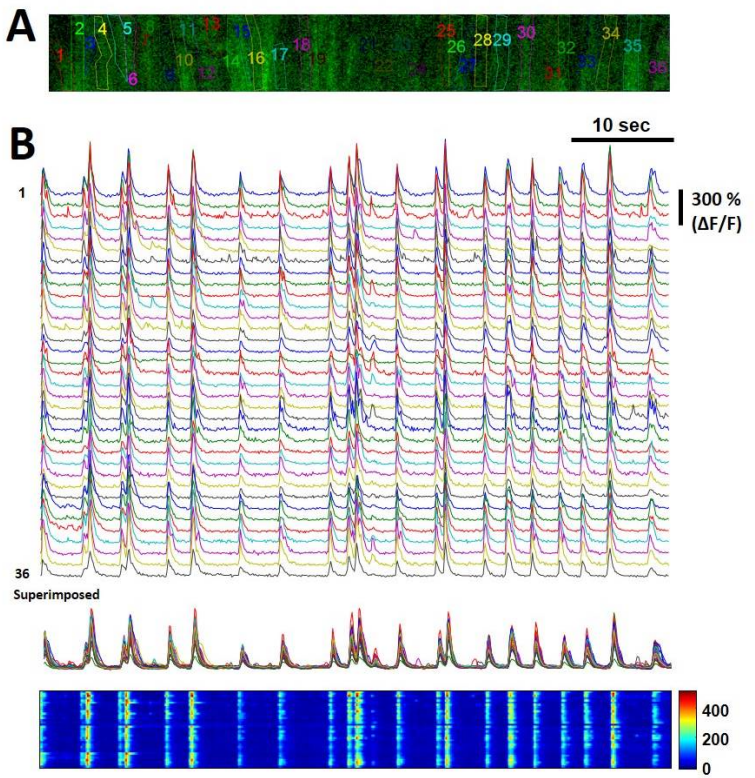
A
B
10 sec
300 %
(ΔF/F)
1
36
Superimposed
400
200
0

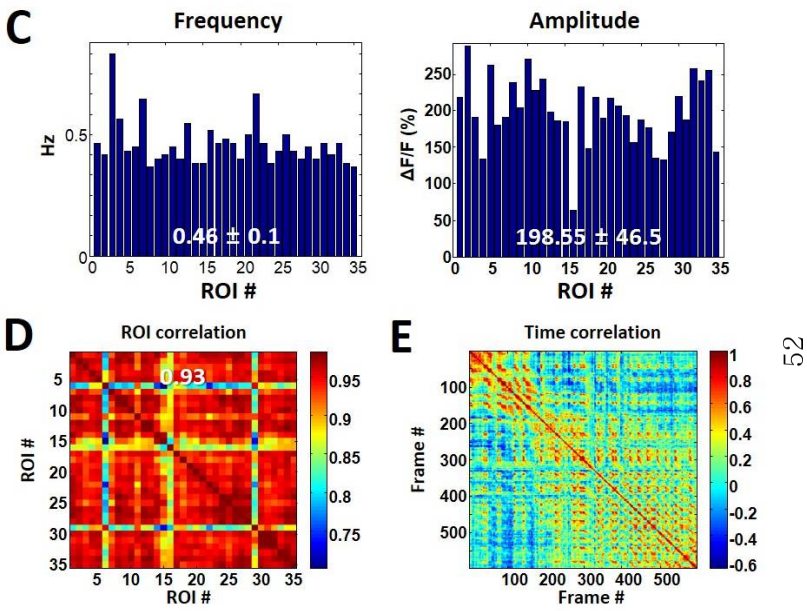
C
Frequency
Amplitude
Hz
ΔF/F (%)
0.46 ± 0.1
198.55 ± 46.5
ROI #
ROI #
D
ROI correlation
0.93
ROI #
ROI #
E
Time correlation
Frame #
Frame #


F

Figure 11. Cerebellar vermis α1-AR blockade causes massive synchrony and tremendously increased amplitudes of PC Ca^{2+} spike. (A) An image showing selection of 36 ROIs (color coded borders) from an image of virally transduced GCaMP6f PC dendrites. (B) PC dendritic Ca^{2+} spike traces from selected ROIs from 60 sec imaging with 16 Hz frame speed. Below, the superimposed traces were shown. The intensity profile matrix was shown at the bottom. (C) The frequencies and amplitudes of selected ROIs were presented as Hz and ΔF/F (%) in the graphs. The average values were presented inside each graph. (D) The synchrony matrix of Pearson's correlation values of each pair of ROIs across all ROIs. X- and Y-axis indicate ROI number (#). The Pearson's correlation values ranges from -1 to 1. -1, 0 and 1 indicate perfect negative correlation, no correlation and perfect positive correlation, respectively. The average of all the Pearson's correlation values from all pairs across all ROIs were presented inside the box. (E) The time correlation matrix which shows the Pearson's correlation values from event patterns of every pair across all imaging frames. X- and Y-axis indicate frame number (#). (F) Representative images of mice injected with prazosin in cerebellar vermis, displaying a kind of anxiety posture (leaning on the wall).

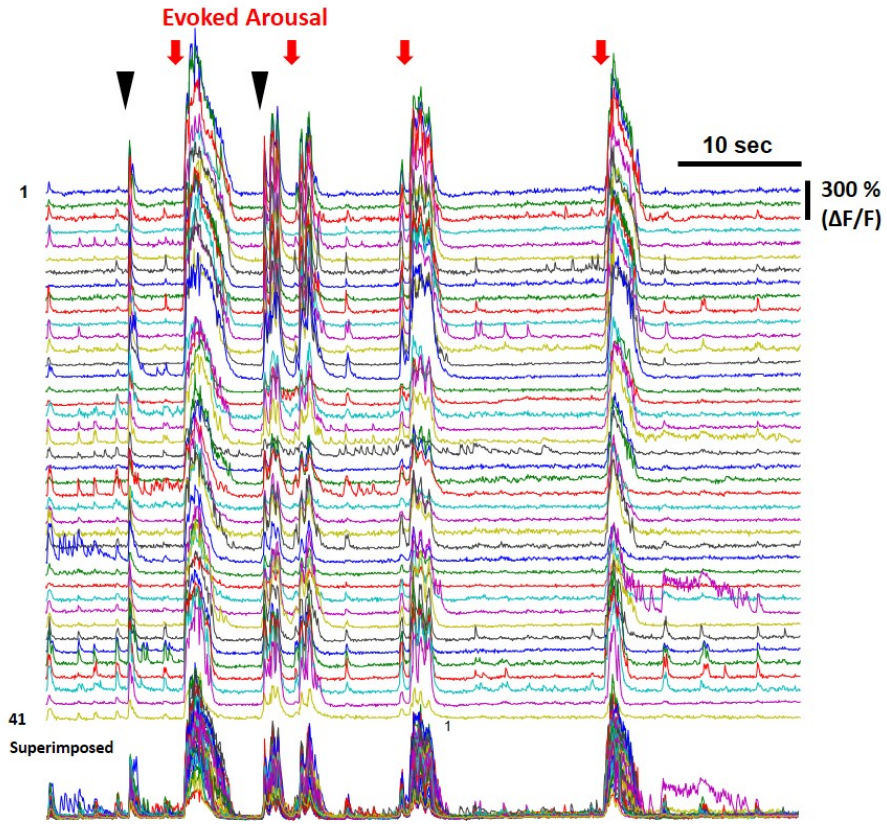

Figure 12. α1-AR blockade in cerebellar vermis results in massive synchrony and tremendously increased amplitudes of PC Ca^{2+} spike. PC dendritic Ca^{2+} spike traces from selected 41 ROIs from 60 sec imaging with 16 Hz frame speed. Red arrows indicate the time point given with arousal stimuli. Black arrow heads represent spontaneous arousal. Shown below is the superimposed traces which show almost perfect co activation of all ROIs.

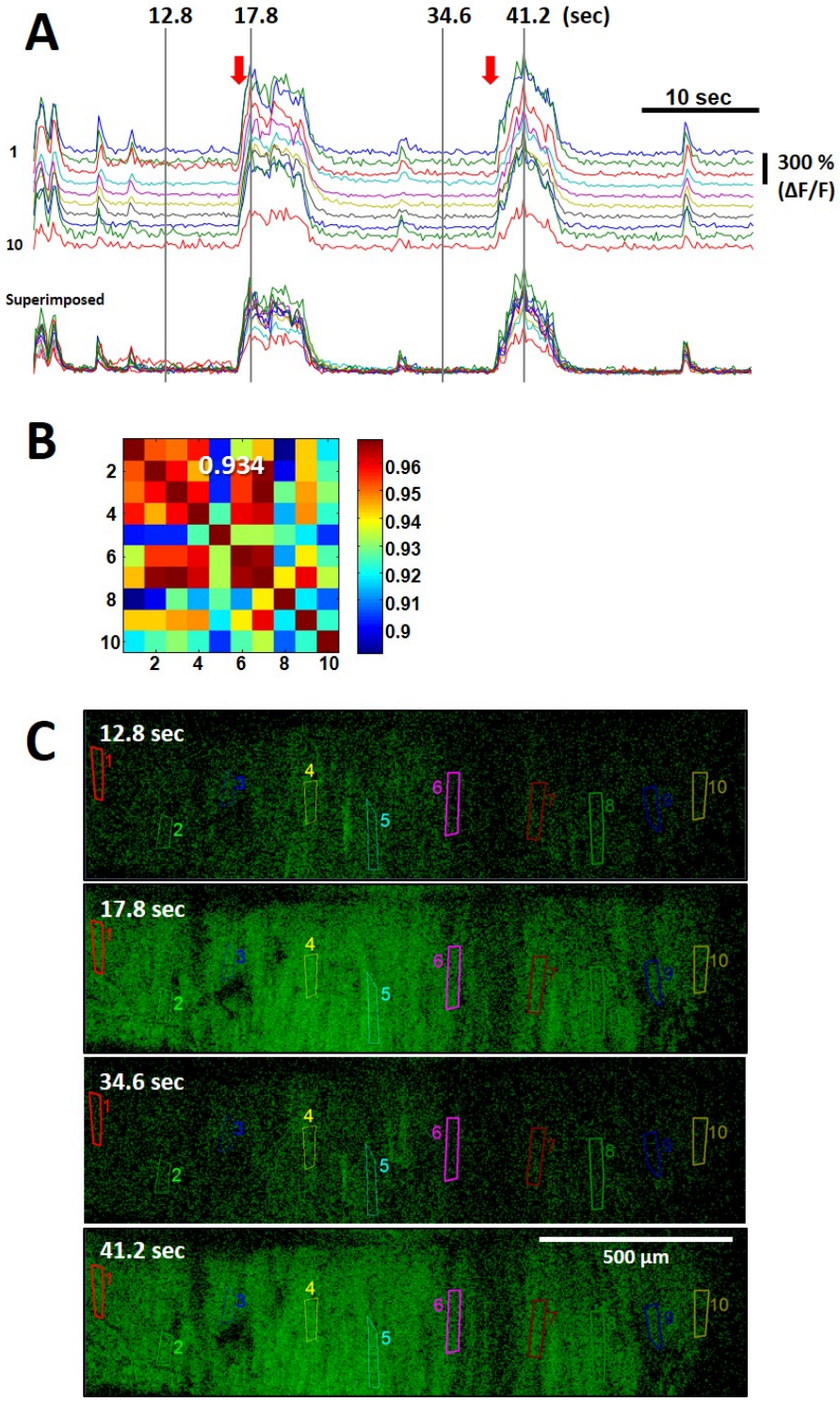
A
12.8
17.8
34.6
41.2 (sec)
10 sec
1
10
300 %
(ΔF/F)
Superimposed
B
0.934
2
4
6
8
10
0.96
0.95
0.94
0.93
0.92
0.91
0.9
C
12.8 sec
17.8 sec
34.6 sec
41.2 sec
500 μm

Figure 13. Prazosin-induced massive synchrony of PC dendritic Ca^{2+} signal spans through whole cerebellar vermis.

(A) PC dendritic Ca^{2+} signal traces from selected 10 ROIs at interval of 160-170 μm from large field imaging with 5× lens. 60 sec imaging with 16 Hz frame speed. Below, the superimposed traces were shown. (B) The synchrony matrix of Pearson's correlation values of each pair of ROIs across the 10 ROIs. X- and Y-axis indicate ROI number (#). The average of all the Pearson's correlation values from all pairs across all ROIs were presented inside the box. (C) Representative images of Ca^{2+} imaging fields at indicated time points, 12.8, 17.8, 34.6 and 41.2 sec.

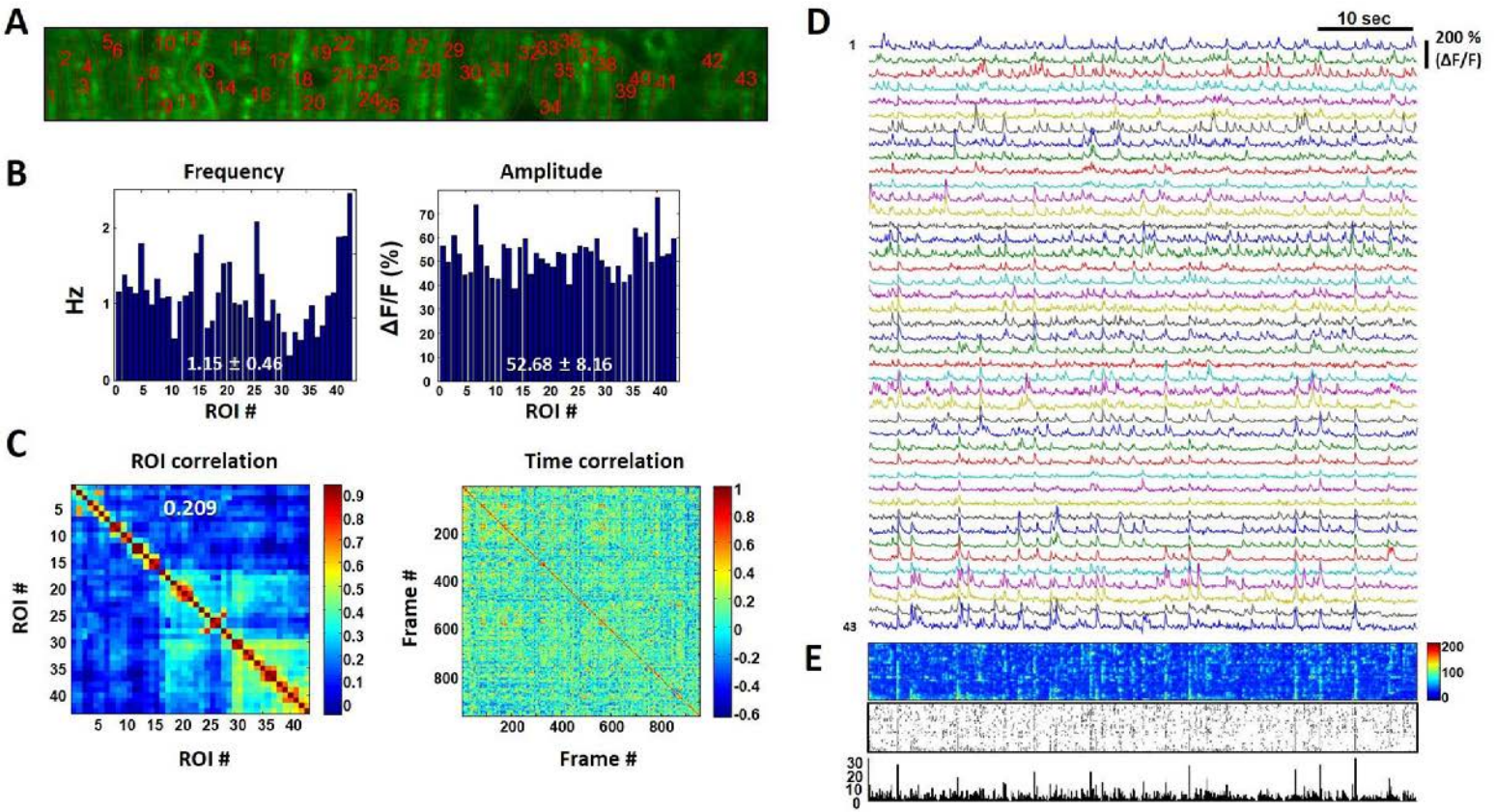
A
B
Frequency
Amplitude
Hz
ΔF/F (%)
1.15 ± 0.46
52.68 ± 8.16
ROI #
C
ROI correlation
Time correlation
0.209
ROI #
Frame #
D
10 sec
200 %
(ΔF/F)
E

Figure14. β-adrenoreceptor Blockade by Propanolol Does Not Severely Affect PC Network Activity.

(A) A high resolution reference image displaying the selection of 43 ROIs (red borders) PC dendrites GCaMP6f imaging field. (B) The frequencies and amplitudes of selected ROIs were presented as Hz and ΔF/F (%) in the graphs. The average values were presented inside each graph. (C) The synchrony matrix of Pearson's correlation values of every pair of ROIs across all ROIs. X- and Y-axis indicate ROI number (#). The average of all the Pearson's correlation values from all pairs across all ROIs were presented inside the box (Left). The time correlation matrix showing the Pearson's correlation values from event patterns of every pair across all imaging frames (Right). X- and Y-axis indicate frame number (#). (D) PC dendritic Ca^{2+} signal traces of selected ROIs during 60 sec. (E) The intensity profile of the PC Ca^{2+} traces reflecting events and their amplitudes (top). Event cumulative (E.C.) plot (middle) and co-activation plot are shown at the middle and bottom.

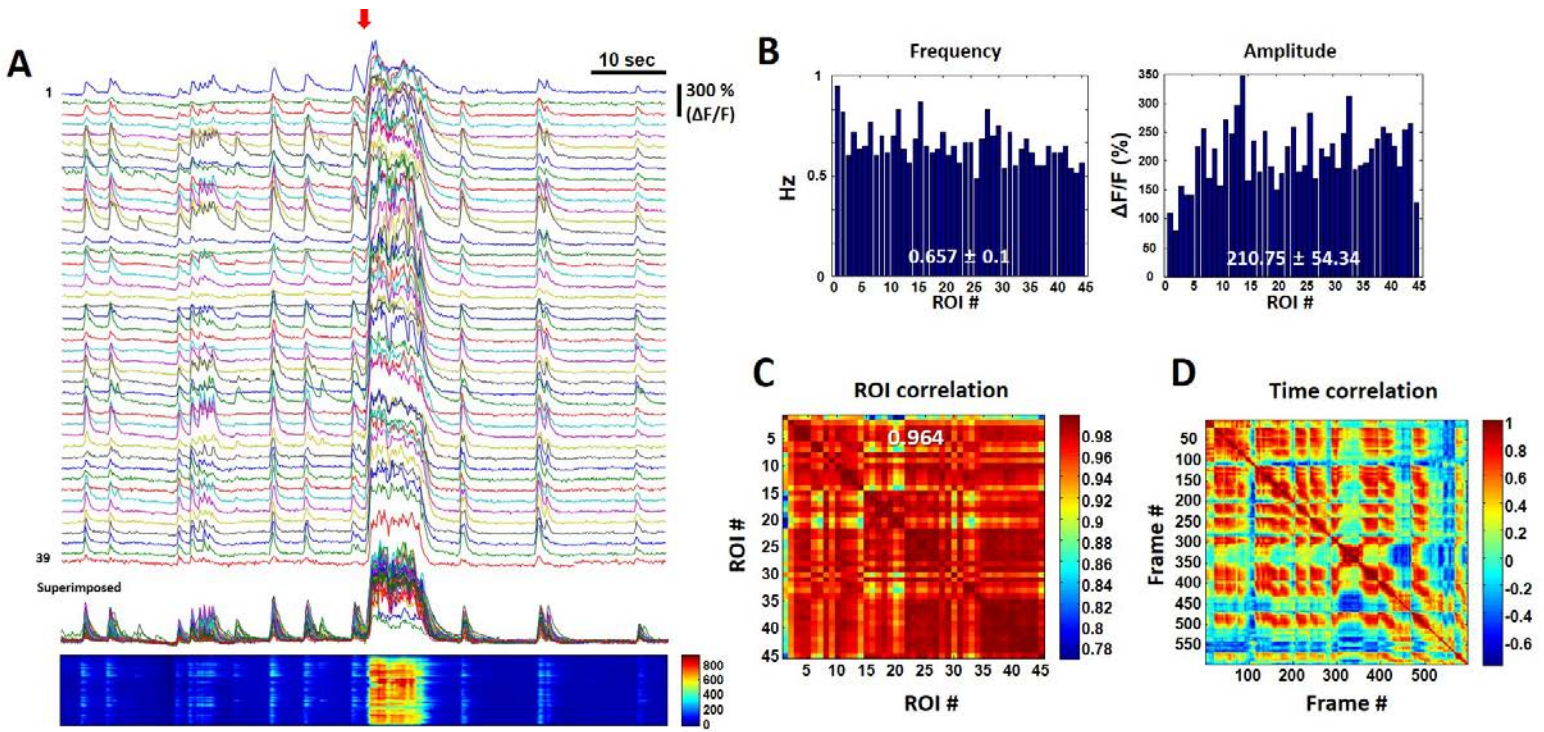
A
10 sec
300 %
(ΔF/F)
1
39
Superimposed
800
600
400
200
0
B
Frequency
Hz
0.657 ± 0.1
ROI #
Amplitude
ΔF/F (%)
210.75 ± 54.34
ROI #
C
ROI correlation
0.964
ROI #
ROI #
D
Time correlation
Frame #
Frame #

Figure 15. Cerebellar vermis glial GABA channel Best1 blockade by NPPB causes massive synchrony and tremendously increased amplitudes of PC Ca^{2+} spike.

(A) PC dendritic Ca^{2+} spike traces from 39 ROIs from 60 sec imaging with 16 Hz frame speed. Below, the superimposed traces were shown. The intensity profile matrix was shown at the bottom. (B) The frequencies and amplitudes of selected ROIs were presented as Hz and ΔF/F (%) ± SD in the graphs. The average values were presented inside each graph. (C) The synchrony matrix of Pearson's correlation values of each pair of ROIs across all ROIs. X- and Y-axis indicate ROI number (#). The average of all the Pearson's correlation values from all pairs among all ROIs was presented inside the box. (D) The time correlation matrix which shows the Pearson's correlation values from event patterns of every pair across all imaging frames. X- and Y-axis indicate frame number (#).

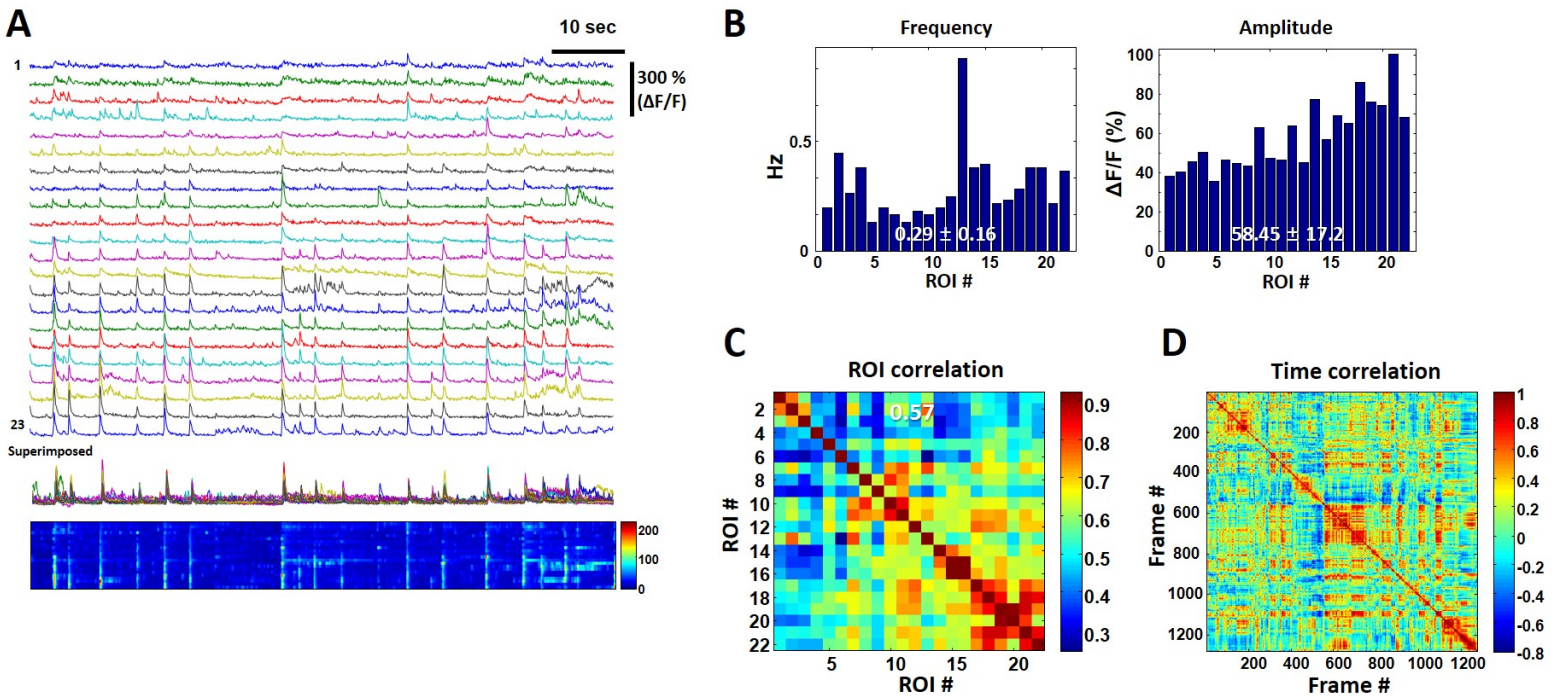
A
10 sec
1
300 %
(ΔF/F)
23
Superimposed
200
100
0
B
Frequency
Hz
0.5
0
0.29 ± 0.16
0
5
10
15
20
ROI #
Amplitude
ΔF/F (%)
100
80
60
40
20
0
58.45 ± 17.2
ROI #
C
ROI correlation
0.57
ROI #
2
4
6
8
10
12
14
16
18
20
22
5
10
15
20
0.9
0.8
0.7
0.6
0.5
0.4
0.3
D
Time correlation
Frame #
200
400
600
800
1000
1200
1
0.8
0.6
0.4
0.2
0
-0.2
-0.4
-0.6
-0.8

Figure 16. NFA injection into cerebellar vermis causes abnormal PC activity and increased synchrony.

(A) PC dendritic Ca^{2+} spike traces from 23 ROIs from 60 sec imaging with 16 Hz frame speed. Below, the superimposed traces and the intensity profile matrix were shown at the bottom. (B) The frequencies and amplitudes of selected ROIs were presented as Hz and $\Delta F/F$ (%) ± SD in the graphs. The average values were presented inside each graph. (C) The synchrony matrix of Pearson's correlation values of each pair of ROIs across all ROIs. X- and Y-axis indicate ROI number (#). The average of all the Pearson's correlation values from all pairs among all ROIs was presented inside the box. (D) The time correlation matrix showing the Pearson's correlation values from event patterns of every pair across all imaging frames. X- and Y-axis indicate frame number (#).

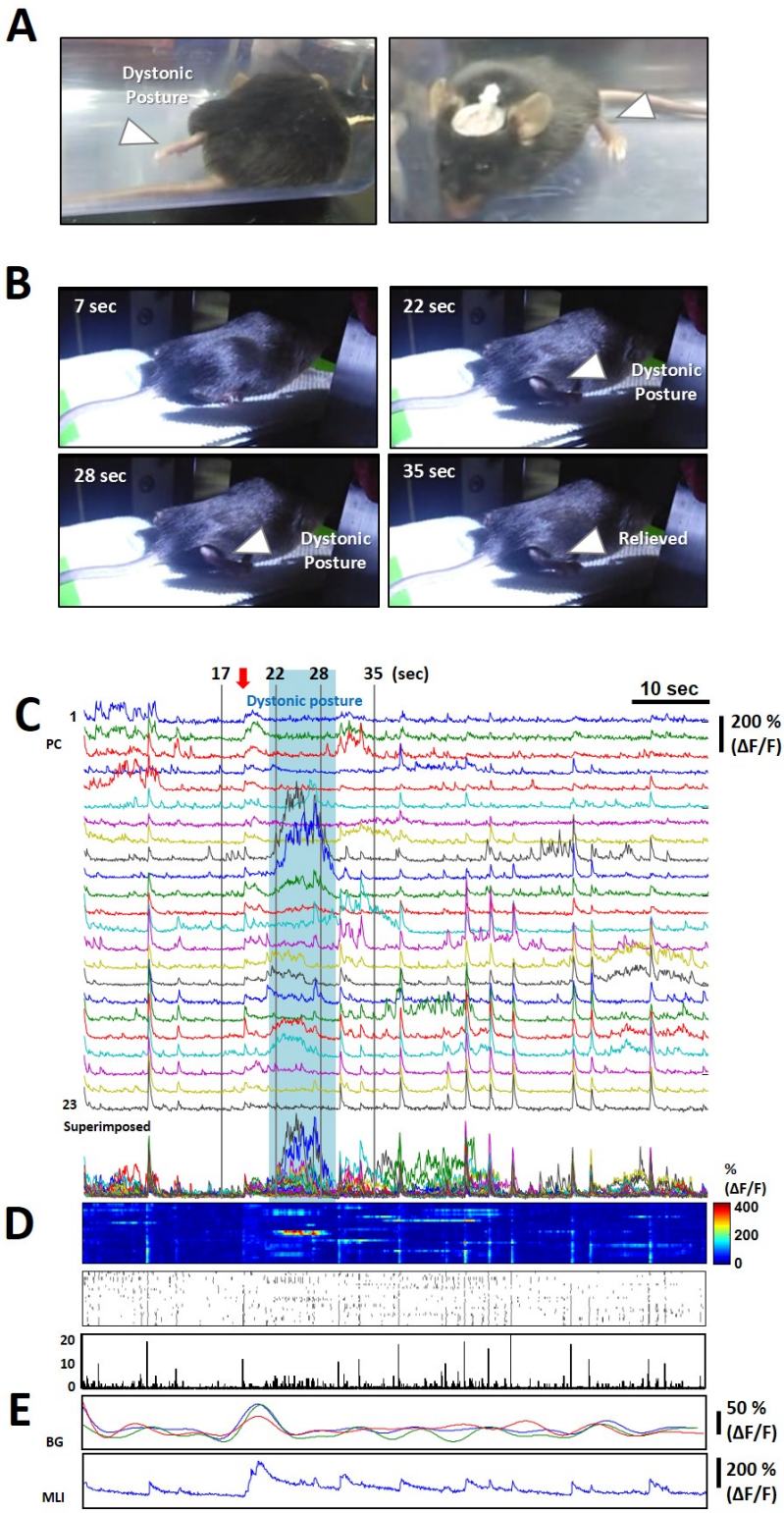
A
Dystonic
Posture
B
7 sec
22 sec
Dystonic
Posture
28 sec
Dystonic
Posture
35 sec
Relieved
C
17
22
28
35 (sec)
Dystonic posture
10 sec
1
PC
200 %
(ΔF/F)
23
Superimposed
%
(ΔF/F)
400
200
0
D
20
10
0
E
BG
50 %
(ΔF/F)
MLI
200 %
(ΔF/F)

Figure 17. Cerebellar vermis injection of NFA causes dystonic posture during which coincides with burst activity of PC Ca^{2+} spikes.

(A) Representative pictures of mice presenting dystonic postures, indicated by white arrow heads, 20 min after injection of NFA. (B) Snapshots from simultaneous video recording of the mouse at resting (7 sec), while experiencing dystonic posture (at 22 and 28 sec) and after relieved (35 sec) The dystonic posture was indicated by white arrow heads. (C) PC dendritic Ca^{2+} spike traces from 23 ROIs from 16 Hz imaging for 60 sec. The superimposed traces were shown below. The time the mouse presents dystonic posture was indicated by light blue box. The four vertical lines at 17, 22, 28 and 35 sec represent the movie frames at which snapshots were presented in B. (D) The intensity profile plot, the event cumulative plot and the co-activation profile plot were shown. (E) The BG Ca^{2+} intensity traces were presented after signal processing of low-pass filtering and Gaussian smoothing. A single MLI's trace was depicted below.

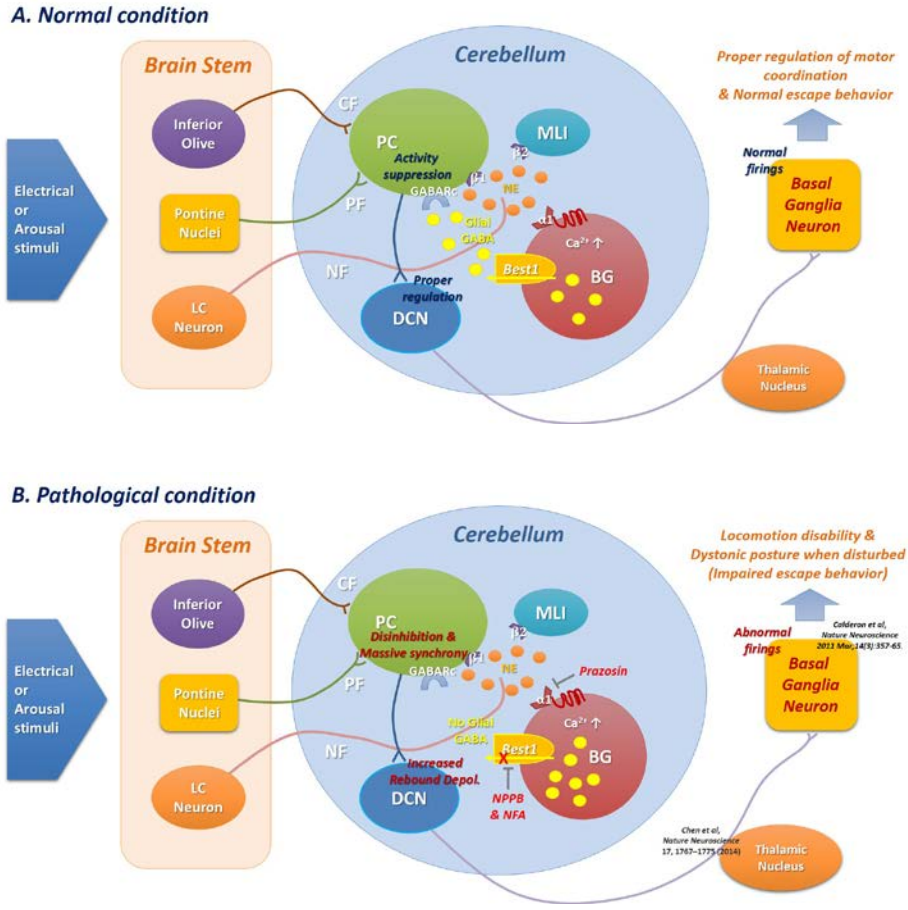
A. Normal condition
Brain Stem
Cerebellum
Inferior Olive
Pontine Nuclei
LC Neuron
Electrical or Arousal stimuli
CF
PF
NF
PC
Activity suppression
MLI
GABARc
NE
Glial GABA
Ca2+ ↑
Best1
BG
Proper regulation
DCN
Proper regulation of motor coordination & Normal escape behavior
Normal firings
Basal Ganglia Neuron
Thalamic Nucleus
B. Pathological condition
Brain Stem
Cerebellum
Inferior Olive
Pontine Nuclei
LC Neuron
Electrical or Arousal stimuli
CF
PF
NF
PC
Disinhibition & Massive synchrony
MLI
GABARc
NE
Prazosin
No Glial GABA
Ca2+ ↑
Best1
BG
Increased Rebound Depol.
DCN
NPPB & NFA
Locomotion disability & Dystonic posture when disturbed (Impaired escape behavior)
Abnormal firings
Basal Ganglia Neuron
Thalamic Nucleus

Figure 18. Summary: Normal and pathological condition by α1-AR or Best1 blockade in cerebellum.

(A) The normal condition is the state in which cerebellum is able to deal with inputs by balancing the excitatory and inhibitory cues. During resting state, BG may release GABA tonically possibly in response to tonic release of norepinephrine (NE), generating the membrane excitability which allows to present proper synchrony and output to deep cerebellar nuclei (DCN). The animal will finally show normal posture. During arousal, the inputs will be transmitted to cerebellum through brainstem, the main gate of cerebellar inputs, which comprise inferior olive (IO), pontine nuclei (PN) and locus coeruleus (LC), each stretching axons into cerebellum as climbing fiber (CF), parallel fiber (PF) and noradrenergic fiber (NF). For proper regulation of PC activity, the sole output of the cerebellum, NF, in combination with molecular layer interneuron (MLI), would serve as an important inhibitory role to avoid abnormal firings. The resulting typical outputs of DCN and normal firing of basal ganglia neurons will promote normal motor coordination and escape behavior. (B) Blockade of α1-AR or Best1 will produce a pathological condition in which inhibitory circuit is damaged due to the absence of tonic and Ca^{2+}-dependent phasic GABA release. The outcome is disinhibition, massive synchrony and sometimes burst activity of PC. It will in turn greatly augment DCN output by aberrantly driving up the rebound depolarization, causing abnormal firings in basal ganglia neurons. Consequently, the animal will experience locomotion disability and dystonic posture when disturbed. PC, Purkinje cell; BG, Bergmann glia; MLI, Molecular layer interneuron; DCN, Deep cerebellar nuclei; PF, Parallel fiber; NF, noradrenergic fiber; NE, norepinephrine.

DISCUSSION

The present study provides a series of novel observations encompassing the regulatory mechanism of interaction between BG and PC by LC-derived NE and its consequences in cerebellar output and motor coordination. To summarize, 1) in anesthetized mice, the peripheral noxious stimulation was shown to reliably induce Ca^{2+} excitation in BG through LC-driven α1-AR activation and it was accompanied by the suppression of PC Ca^{2+} spike. 2) Also in awake behaving mice, BGCR coincided with PC suppression in response to arousal stimuli. 3) The pharmacological approach which employed the blockade of α1-AR other than β-AR caused tremendously increased response and massive synchrony of PC dendritic Ca^{2+} spike. 4) Interestingly, the blockade of glial GABA channel Best1 exerted the same effect with that of α1-AR, abnormally increasing both network synchrony and amplitudes of PC Ca^{2+} spikes while decreasing the spike rates. 5) Remarkably, pharmacological inhibition of both molecules gave rise to PC burst activity in response to arousal stimuli and its duration well corresponded with dystonic posture presentation of mice. Collectively, these results implicate BG as an active participant which critically modulates cerebellar sole output, PC, and cerebellum-dependent motor coordination, ultimately suggesting α1-AR or Best1 mediated GABA release as risk factors for motor disease such as Parkinson's disease and dystonia.

Robust Bergmann glia Ca^{2+} activation by arousal-like stimuli in anesthetized mice

In this study, cutaneous ES was shown, for the first time, to trigger Ca^{2+} transients in BG of cerebellar cortex and it was not specific to receptive field in anesthetized mice (Figure 1). The same stimulation also triggered astrocyte Ca^{2+} transients in somatosensory cortex (Figure 3). Considering the BGCR amplitude is dependent on the intensity, duration and frequency of the stimulation, it can be inferred that the activity of LC neurons respond to such parameters which determine the amount of NE release. Definitely, this process relies on the peripheral and central synaptic transmission as tested by lidocaine and TTX administration (Figure 2). Also, ES-evoked BGCR is almost exclusively dependent on α1-AR signaling and other receptors related to BG Ca^{2+} transients obviously have limited effects (Figure 4). Though the activation of AMPA receptor, mGluR1 and P2Y are known to trigger Ca^{2+} influx in BG, literatures indicate that the down-stream signaling molecules are different between them and the ones related to α1-AR. The present results verify that the BGCR is purely mediated by α1-AR activation. So, what is the function of BG Ca^{2+} excitation by noradrenergic drive?

Providing mechanistic insights of noradrenergic regulation in cerebellum with technical advances in multi-cell type Ca^{2+} imaging combined with cannula local drug delivery system

Many reports have described the effect of NE in cerebellar circuits in which it activates β-AR and α-ARs to down-regulate PC firing rates (Carey and Regehr, 2009; Cheun and Yeh, 1992; Herold et al., 2005; Saitow et al., 2000). However, majority of the studies was performed with *in vitro* slice which does not represent whole circuit in and out cerebellum or with *in vivo* field recording which does not purely identify PC activity, which means the results inevitably include non-physiological contexts. Two-photon microscopy has provided an effective means to reveal *in vivo* phenomenon in an intact brain of anesthetized and awake behaving mice as well. PC specific imaging was achieved by cre-dependent expression of GCaMP6f in pcp2-cre TG mice (Figure 5). From this, the PC dendritic Ca^{2+} spike activity was successfully recorded, revealing the suppression of PC activity by peripheral noxious stimulation (Figure 6) and arousal stimuli such as tail-pulling or whisker touching (Figure 9) in anesthetized mice and awake behaving mice, respectively.

Next, the simultaneous imaging of glia and neurons was accomplished by general expression of CAG promoter-driven GCaMP6f expression (Figure 7). Though there appear no expressions in BG, they exhibited Ca^{2+} excitation in response to physiological stimuli. Hence, using such a powerful system, the regulation of PC and BG by NE was monitored at the same time. Normally, they display moderate synchronized dendritic Ca^{2+} activity with around 1 Hz during resting state (Figure 8). However, the phasic suppression of PC activity was apparent while BG mobilize intracellular Ca^{2+} in response to startle stimuli (Figure 9).

The next question will be whether BG Ca^{2+} excitation is indeed functionally associated with PC suppression during peripheral stimulation. To answer such a compelling question, pharmacological approaches were exploited using cannula during two-photon Ca^{2+} imaging. Former two-photon imaging studies in cerebellar cortex accompanying local drug application only performed intraperitoneal injection or superficial cortical application (Nimmerjahn et al., 2009; Paukert et al., 2014). However, this system can be hardly applicable to chronic window on which glass cover slip is firmly glued. Also, this is not appropriate for simultaneously observing the behavior of drug effects during imaging. Therefore, a special delivery system with a cannula installed while chronic window is prepared for carrying out cerebellar drug injection during imaging (Figure 10A). This is a quite effective system capable of wash-out of drugs in 1 or 2 days post experiment. Also, SR101 is co-injected to ensure the delivery and label BG (Figure 10B). Owing to such a system, various drugs could be tested for ongoing studies.

Bergmann Glia as a signaling nexus between α1-adrenergic signaling and best1-mediated GABAergic transmission

Other than β-AR blockers, cerebellar vermis injection of α1-AR blocker terazosin or prazosin was shown to cause severely impaired exploratory behavior (Stone et al., 2004). However, the cell level mechanism and specific behaviors related (i.e., motor coordination) remained to be understood. Present result indicates that prazosin induces massive synchrony with increased amplitudes of PC dendritic Ca^{2+} spikes during resting and arousal state (Figure

11 and 12). The synchrony derives from electrical coupling of inferior olivary neurons through gap junctions and falls off 100-200 μm mediolaterally on cerebellar cortex, forming microbands of PC co-activation (Ozden et al., 2009; Schultz et al., 2009). Very interestingly, however, the synchrony during α1-AR blockade spans though ~ 1.6 mm parasagittal area which is most of vermis region (Figure 13). How is the massive synchrony generated then?

Assuming that α1-AR exerts strong inhibitory drives in cerebellum in response to NE, I should pay attention to a recent study demonstrating tonic GABA release through direct permeation by the Ca^{2+}-activated chloride channel Best1 of BG (Lee et al., 2010). More recently, Ca^{2+}-dependent phasic GABA release in response to protease activated receptor agonist was described (Yoon et al., 2014). Thus, the best1 blockers NPPB and NFA were tested for Ca^{2+} imaging. Surprisingly, NPPB effect was very similar with that of prazosin: abnormally elevated amplitudes and synchrony of PC activity. The results strongly indicate that the outcomes of α1-AR and Best1 action should converge on the same signaling pathway directing disinhibition and massive synchrony of PC. Hence, it can be proposed that as a cerebellar signaling nexus, BG serves as receiving noradrenergic input and representing its GABAergic transmission (Figure 18).

More remarkably, in the presence of another Best1 blocker NFA, mice showed abnormal postures upon arousal stimuli, during which significant number of PC dendrites displayed burst activity of Ca^{2+} transients (Figure 17). Since such a coincidence was clear, I sought for some disease relevance and any relationship between the burst activity and the abnormal behavior.

Implications of glial α1-AR and GABA as risk factors for motor diseases

Dystonias, as the third most movement disorder, are featured by involuntary movements and abnormal postures due to co-contraction of agonizing and antagonizing muscles (Breakefield et al., 2008). Although dystonias traditionally have been regarded as a disease of basal ganglia, recent studies have suggested the involvement of cerebellum in the disease process (Filip et al., 2013). In an animal model of rapid-onset Dystonia Parkinsonism (RDP), the cerebellum was suggested to be the primary cause of dystonia, inducing abnormal function of basal ganglia (Calderon et al., 2011). A following study demonstrated the presence of di-synaptic pathway through which cerebellum rapidly modulate basal ganglia activity, relaying aberrant signals to induce dystonia at pathological conditions (Chen et al., 2014). The present study reports abnormally increased PC network synchrony and enhanced activity magnitudes at resting and during arousal upon α1-AR or glial GABA channel blockade (Figure 13, 14 and 16). It can be inferred that abnormally high Ca^{2+} activity in a large field with massive synchrony will be translated as aberrant activities in DCN. It is supported by recent studies describing strong rebound firing of DCN neurons in response to cortical PC input in a strength-dependent manner (Sekirnjak et al., 2003; Witter et al., 2013). Hence, the dystonic posture observed in mice injected with best1 blockers in cerebellar vermis is thought to result from aberrant rebound firings of DCN and relayed abnormal activities in basal ganglia (Figure 18). This is interesting that BG modulation results in

abnormal PC activity. Another remarkable finding is the contribution of α1-AR and glial GABA to the pathological condition. This is the first study to implicate BG as a prominent regulator of PC dendritic Ca^{2+} network synchrony and eventually movement diseases such as dystonia. It will be helpful to carry out genetic or histological etiology study to better understand dystonias, targeting the molecules related to α1-adrenergic signaling or glial GABA transmission.

Conclusion

In conclusion, the present study has revealed an important noradrenergic inhibitory signaling by alpha1-AR in BG, where PC is down-regulated by inhibitory gliotransmission. This study also suggests that the problems in such system will be an important cause in pathological conditions of dystonia, presented by aberrant PC activity that triggers abnormal activities in DCN and then basal ganglia in order.

REFERENCES

Abbott, L.C., and Sotelo, C. (2000). Ultrastructural analysis of catecholaminergic innervation in weaver and normal mouse cerebellar cortices. The Journal of comparative neurology *426*, 316-329.

Aston-Jones, G., and Cohen, J.D. (2005). An integrative theory of locus coeruleus-norepinephrine function: adaptive gain and optimal performance. Annual review of neuroscience *28*, 403-450.

Basile, A.S., and Dunwiddie, T.V. (1984). Norepinephrine elicits both excitatory and inhibitory responses from Purkinje cells in the in vitro rat cerebellar slice. Brain research *296*, 15-25.

Bekar, L.K., He, W., and Nedergaard, M. (2008). Locus coeruleus alpha-adrenergic-mediated activation of cortical astrocytes in vivo. Cerebral cortex *18*, 2789-2795.

Bickford-Wimer, P., Pang, K., Rose, G.M., and Gerhardt, G.A. (1991). Electrically-evoked release of norepinephrine in the rat cerebellum: an in vivo electrochemical and electrophysiological study. Brain research *558*, 305-311.

Bloom, F.E., Hoffer, B.J., and Siggins, G.R. (1971). Studies on norepinephrine-containing afferents to Purkinje cells of art cerebellum. I. Localization of the fibers and their synapses. Brain research *25*, 501-521.

Breakefield, X.O., Blood, A.J., Li, Y., Hallett, M., Hanson, P.I., and Standaert, D.G. (2008). The pathophysiological basis of dystonias. Nature reviews Neuroscience *9*, 222-234.

Brockhaus, J., and Deitmer, J.W. (2002). Long-lasting modulation of synaptic input to Purkinje neurons by Bergmann glia stimulation in rat brain slices. The Journal of physiology *545*, 581-593.

Calderon, D.P., Fremont, R., Kraenzlin, F., and Khodakhah, K. (2011). The neural substrates of rapid-onset Dystonia-Parkinsonism. Nature neuroscience *14*, 357-365.

Carey, M.R., and Regehr, W.G. (2009). Noradrenergic control of associative synaptic plasticity by selective modulation of instructive signals. Neuron *62*, 112-122.

Carrillo, J., Cheng, S.Y., Ko, K.W., Jones, T.A., and Nishiyama, H. (2013). The long-term structural plasticity of cerebellar parallel fiber axons and its modulation by motor learning. The Journal of neuroscience : the official journal of the Society for Neuroscience *33*, 8301-8307.

Chen, C.H., Fremont, R., Arteaga-Bracho, E.E., and Khodakhah, K. (2014). Short latency cerebellar modulation of the basal ganglia. Nature neuroscience *17*, 1767-1775.

Chen, T.W., Wardill, T.J., Sun, Y., Pulver, S.R., Renninger, S.L., Baohan, A., Schreiter, E.R., Kerr, R.A., Orger, M.B., Jayaraman, V., *et al.* (2013).

Ultrasensitive fluorescent proteins for imaging neuronal activity. Nature *499*, 295-300.
Cheun, J.E., and Yeh, H.H. (1992). Modulation of GABAA receptor-activated current by norepinephrine in cerebellar Purkinje cells. Neuroscience *51*, 951-960.
De Gruijl, J.R., Hoogland, T.M., and De Zeeuw, C.I. (2014). Behavioral correlates of complex spike synchrony in cerebellar microzones. The Journal of neuroscience : the official journal of the Society for Neuroscience *34*, 8937-8947.
Farrant, M., and Nusser, Z. (2005). Variations on an inhibitory theme: phasic and tonic activation of GABA(A) receptors. Nature reviews Neuroscience *6*, 215-229.
Filip, P., Lungu, O.V., and Bares, M. (2013). Dystonia and the cerebellum: a new field of interest in movement disorders? Clinical neurophysiology : official journal of the International Federation of Clinical Neurophysiology *124*, 1269-1276.
Fine, E.J., Ionita, C.C., and Lohr, L. (2002). The history of the development of the cerebellar examination. Seminars in neurology *22*, 375-384.
Gonzalez, M.M., and Aston-Jones, G. (2006). Circadian regulation of arousal: role of the noradrenergic locus coeruleus system and light exposure. Sleep *29*, 1327-1336.
Herold, S., Hecker, C., Deitmer, J.W., and Brockhaus, J. (2005). alpha1-Adrenergic modulation of synaptic input to Purkinje neurons in rat cerebellar brain slices. Journal of neuroscience research *82*, 571-579.
Hirono, M., and Obata, K. (2006). Alpha-adrenoceptive dual modulation of inhibitory GABAergic inputs to Purkinje cells in the mouse cerebellum. Journal of neurophysiology *95*, 700-708.
Hoogland, T.M., Kuhn, B., and Wang, S.S. (2011). Preferential loading of bergmann glia with synthetic acetoxymethyl calcium dyes. Cold Spring Harbor protocols *2011*, 1228-1231.
Kang, J., Jiang, L., Goldman, S.A., and Nedergaard, M. (1998). Astrocyte-mediated potentiation of inhibitory synaptic transmission. Nature neuroscience *1*, 683-692.
Kim, S.K., and Nabekura, J. (2011). Rapid synaptic remodeling in the adult somatosensory cortex following peripheral nerve injury and its association with neuropathic pain. The Journal of neuroscience : the official journal of the Society for Neuroscience *31*, 5477-5482.
Kimoto, Y., Satoh, K., Sakumoto, T., Tohyama, M., and Shimizu, N. (1978). Afferent fiber connections from the lower brain stem to the rat cerebellum by the horseradish peroxidase method combined with MAO staining, with special reference to noradrenergic neurons. Journal fur Hirnforschung *19*, 85-100.
Kirischuk, S., Tuschick, S., Verkhratsky, A., and Kettenmann, H. (1996). Calcium signalling in mouse Bergmann glial cells mediated by alpha1-

adrenoreceptors and H1 histamine receptors. The European journal of neuroscience *8*, 1198-1208.
Kitamura, K., and Hausser, M. (2011). Dendritic calcium signaling triggered by spontaneous and sensory-evoked climbing fiber input to cerebellar Purkinje cells in vivo. The Journal of neuroscience : the official journal of the Society for Neuroscience *31*, 10847-10858.
Kulik, A., Haentzsch, A., Luckermann, M., Reichelt, W., and Ballanyi, K. (1999). Neuron-glia signaling via alpha(1) adrenoceptor-mediated Ca(2+) release in Bergmann glial cells in situ. The Journal of neuroscience : the official journal of the Society for Neuroscience *19*, 8401-8408.
Lalo, U., Palygin, O., Rasooli-Nejad, S., Andrew, J., Haydon, P.G., and Pankratov, Y. (2014). Exocytosis of ATP from astrocytes modulates phasic and tonic inhibition in the neocortex. PLoS biology *12*, e1001747.
Lawlor, P.A., Bland, R.J., Mouravlev, A., Young, D., and During, M.J. (2009). Efficient gene delivery and selective transduction of glial cells in the mammalian brain by AAV serotypes isolated from nonhuman primates. Molecular therapy : the journal of the American Society of Gene Therapy *17*, 1692-1702.
Lee, S., Yoon, B.E., Berglund, K., Oh, S.J., Park, H., Shin, H.S., Augustine, G.J., and Lee, C.J. (2010). Channel-mediated tonic GABA release from glia. Science *330*, 790-796.
Moises, H.C., Woodward, D.J., Hoffer, B.J., and Freedman, R. (1979). Interactions of norepinephrine with Purkinje cell responses to putative amino acid neurotransmitters applied by microiontophoresis. Experimental neurology *64*, 493-515.
Muller, T., Moller, T., Berger, T., Schnitzer, J., and Kettenmann, H. (1992). Calcium entry through kainate receptors and resulting potassium-channel blockade in Bergmann glial cells. Science *256*, 1563-1566.
Najafi, F., Giovannucci, A., Wang, S.S., and Medina, J.F. (2014). Sensory-driven enhancement of calcium signals in individual Purkinje cell dendrites of awake mice. Cell reports *6*, 792-798.
Newman, E.A., and Zahs, K.R. (1998). Modulation of neuronal activity by glial cells in the retina. The Journal of neuroscience : the official journal of the Society for Neuroscience *18*, 4022-4028.
Nimmerjahn, A., Mukamel, E.A., and Schnitzer, M.J. (2009). Motor behavior activates Bergmann glial networks. Neuron *62*, 400-412.
Ozden, I., Dombeck, D.A., Hoogland, T.M., Tank, D.W., and Wang, S.S.H. (2012). Widespread State-Dependent Shifts in Cerebellar Activity in Locomoting Mice. Plos One *7*.
Ozden, I., Sullivan, M.R., Lee, H.M., and Wang, S.S. (2009). Reliable coding emerges from coactivation of climbing fibers in microbands of cerebellar Purkinje neurons. The Journal of neuroscience : the official journal of the Society for Neuroscience *29*, 10463-10473.

Parfitt, K.D., Freedman, R., and Bickford-Wimer, P.C. (1988). Electrophysiological effects of locally applied noradrenergic agents at cerebellar Purkinje neurons: receptor specificity. Brain research *462*, 242-251.
Paukert, M., Agarwal, A., Cha, J., Doze, V.A., Kang, J.U., and Bergles, D.E. (2014). Norepinephrine controls astroglial responsiveness to local circuit activity. Neuron *82*, 1263-1270.
Pertovaara, A. (2006). Noradrenergic pain modulation. Progress in neurobiology *80*, 53-83.
Poskanzer, K.E., and Yuste, R. (2011). Astrocytic regulation of cortical UP states. Proceedings of the National Academy of Sciences of the United States of America *108*, 18453-18458.
Ramnani, N. (2006). The primate cortico-cerebellar system: anatomy and function. Nature reviews Neuroscience *7*, 511-522.
Saitow, F., Satake, S., Yamada, J., and Konishi, S. (2000). beta-adrenergic receptor-mediated presynaptic facilitation of inhibitory GABAergic transmission at cerebellar interneuron-Purkinje cell synapses. Journal of neurophysiology *84*, 2016-2025.
Sasaki, T., Beppu, K., Tanaka, K.F., Fukazawa, Y., Shigemoto, R., and Matsui, K. (2012). Application of an optogenetic byway for perturbing neuronal activity via glial photostimulation. Proceedings of the National Academy of Sciences of the United States of America *109*, 20720-20725.
Schultz, S.R., Kitamura, K., Post-Uiterweer, A., Krupic, J., and Hausser, M. (2009). Spatial pattern coding of sensory information by climbing fiber-evoked calcium signals in networks of neighboring cerebellar Purkinje cells. The Journal of neuroscience : the official journal of the Society for Neuroscience *29*, 8005-8015.
Sekirnjak, C., Vissel, B., Bollinger, J., Faulstich, M., and du Lac, S. (2003). Purkinje cell synapses target physiologically unique brainstem neurons. The Journal of neuroscience : the official journal of the Society for Neuroscience *23*, 6392-6398.
Stone, E.A., Lin, Y., Ahsan, R., and Quartermain, D. (2004). Gross mapping of alpha1-adrenoceptors that regulate behavioral activation in the mouse brain. Behavioural brain research *152*, 167-175.
Strick, P.L., Dum, R.P., and Fiez, J.A. (2009). Cerebellum and nonmotor function. Annual review of neuroscience *32*, 413-434.
Thrane, A.S., Rangroo Thrane, V., Zeppenfeld, D., Lou, N., Xu, Q., Nagelhus, E.A., and Nedergaard, M. (2012). General anesthesia selectively disrupts astrocyte calcium signaling in the awake mouse cortex. Proceedings of the National Academy of Sciences of the United States of America *109*, 18974-18979.
Torres, A., Wang, F., Xu, Q., Fujita, T., Dobrowolski, R., Willecke, K., Takano, T., and Nedergaard, M. (2012). Extracellular Ca(2)(+) acts as a mediator of communication from neurons to glia. Science signaling *5*, ra8.
Wang, F., Xu, Q., Wang, W., Takano, T., and Nedergaard, M. (2012). Bergmann glia modulate cerebellar Purkinje cell bistability via Ca2+ -

dependent K+ uptake. Proceedings of the National Academy of Sciences of the United States of America *109*, 7911-7916.
Waterhouse, B.D., Moises, H.C., and Woodward, D.J. (1980). Noradrenergic modulation of somatosensory cortical neuronal responses to iontophoretically applied putative neurotransmitters. Experimental neurology *69*, 30-49.
Waterhouse, B.D., Moises, H.C., Yeh, H.H., Geller, H.M., and Woodward, D.J. (1984). Comparison of norepinephrine- and benzodiazepine-induced augmentation of Purkinje cell responses to gamma-aminobutyric acid (GABA). The Journal of pharmacology and experimental therapeutics *228*, 257-267.
Waterhouse, B.D., and Woodward, D.J. (1980). Interaction of norepinephrine with cerebrocortical activity evoked by stimulation of somatosensory afferent pathways in the rat. Experimental neurology *67*, 11-34.
Witter, L., Canto, C.B., Hoogland, T.M., de Gruijl, J.R., and De Zeeuw, C.I. (2013). Strength and timing of motor responses mediated by rebound firing in the cerebellar nuclei after Purkinje cell activation. Frontiers in neural circuits *7*, 133.
Xie, L., Kang, H., Xu, Q., Chen, M.J., Liao, Y., Thiyagarajan, M., O'Donnell, J., Christensen, D.J., Nicholson, C., Iliff, J.J.*, et al.* (2013). Sleep drives metabolite clearance from the adult brain. Science *342*, 373-377.
Yoon, B.E., Woo, J., Chun, Y.E., Chun, H., Jo, S., Bae, J.Y., An, H., Min, J.O., Oh, S.J., Han, K.S.*, et al.* (2014). Glial GABA, synthesized by monoamine oxidase B, mediates tonic inhibition. The Journal of physiology.

국문 초록

서론: 청반(LC)에서 유래하는 노르에피네프린은 소뇌를 포함한 뇌의 여러 영역에서 신경세포와 아교세포 조절하여 각성을 하게 하는데에 중요한 역할을 한다. 하지만 소뇌에서 NE 에 의한 신경세포-아교세포의 상호작용과 그것이 각성 과정에서 어떤 생리학적 기능을 하는지에 대해서는 밝혀지지 않았다.

방법: 마취되거나 깨어있는 생쥐 소뇌 충부에서 신경세포와 버그만아교세포, 중강신경세포의 활성을 측정하기 위해 합성 칼슘 표지자 OGB-1 과 칼슘 표지 단백질 GCaMP6f 를 사용해 이광자 현미경 기법을 수행하였고 약물처리기법을 병행하였다. 마취된 생쥐에는 뒷발에 유해 전기자극을 주었고 깨어있는 생쥐에서는 각성 자극을 주며 칼슘영상을 수행하였다.

결과: 마취된 생쥐에서 말초 피하 전기자극을, 깨어 있는 생쥐에서 각성자극을 줄 때 버그만아교세포에서 칼슘유입이 증가함을 관찰하였고, 같은 자극에 의해 퍼킨지세포의 활성이 급격히 감소함을 보았다. 퍼킨지-버그만아교세포 동시 칼슘 영상화 기법을 통해 이 두 결과가 시간적으로 일치함을 증명하였고, 깨어있는 생쥐에서도 각성반응시에 같은 결과를 얻었다. 소뇌 충부 특이적으로 알파아드레노수용체 저해제와 가바통로인 Best1 저해재를 주입시 퍼킨지세포간의 비정상적인 네트워크 동시성과 엄청나게 증가된 반응성을 확인하였다. Best1 저해시 각성자극을 줄 때 퍼킨지세포는 폭발적인 반응을 보이며 이것이 디스토니아의 자세유발과 동시에 일어남을 증명하였다.

결론: 결론적으로, 청반 유래 노르아드레날린은 소뇌에서 퍼킨지세포-버그만아교세포의 상호작용 조절하며, 퍼킨지세포의 활성을 알맞게 억제하여 적절한 퍼킨지세포 출력과 운동제어에서

중요한 역할을 함을 보였으며, 이 과정이 방해 받았을 때 디스토니아와 같은 운동장애가 발생할 수 있음을 보였다.

주요어 : 소뇌, 노르에피네프린, 청반, 칼슘, 버그만아교세포, 퍼킨지세포, 신경교세포상호작용

학 번 : 2010-30609